

# Optimizing Hydrogen Fueling Infrastructure Plans on Freight Corridors for Heavy Duty Fuel Cell Electric Vehicles

*Adam Siekmann, Vivek Sujan, Majbah Uddin, Yuandong Liu, Fei Xie*

## Abstract

The development of a future hydrogen energy economy will require the development of several hydrogen market and industry segments including a hydrogen based commercial freight transportation ecosystem. For a sustainable freight transportation ecosystem, the supporting fueling infrastructure and the associated vehicle powertrains making use of hydrogen fuel will need to be co-established. This paper introduces the OR-AGENT (Optimal Regional Architecture Generation for Electrified National Transportation) tool developed at the Oak Ridge National Laboratory, which has been used to optimize the hydrogen refueling infrastructure requirements on the I-75 corridor for heavy duty (HD) fuel cell electric commercial vehicles (FCEV). This constraint-based optimization model considers existing fueling locations, regional specific vehicle fuel economy and weight, vehicle origin and destination (O-D), vehicle volume by class and infrastructure costs to characterize in-mission refueling requirements for a given freight corridor. The authors applied this framework to determine the ideal public access locations for hydrogen refueling (constrained by existing fueling stations), the minimal viable cost to deploy sufficient hydrogen fuel dispensers, and associated equipment, to accommodate a growing population of hydrogen fuel cell trucks. The framework discussed in this paper can be expanded and applied to a larger interstate system, expanded regional corridor, or other transportation network. This paper is the third in a series of papers that defined the model development to optimize a national hydrogen refueling infrastructure eco-system for heavy duty commercial vehicles.

## Introduction

The development of a future hydrogen energy economy will require the development of several hydrogen market and industry segments including hydrogen based commercial freight transportation ecosystem [Error! Reference source not found.,1,3,4,5]. As more countries and companies commit to a reduction in criteria and greenhouse gas emissions from vehicles to reduce pollution and combat climate change concerns [6,7,8,9,10], there needs to be an aligned strategy to provide the infrastructure to accelerate the adoption of new and emerging vehicle powertrain technologies. This is especially critical for the freight transportation industry where 24% of all transportation generated GHG emissions come from freight truck movement. At present, while R&D into vehicle technologies for the use of electricity or hydrogen as a fuel is rapidly gaining momentum, the challenge in the near term towards sustainable large scale customer adoption remains [Error! Reference source not found.,11]. The rate and pace of technology evolution and how it will affect the energy pathways for commercial transportation and industrial use are dependent on multiple variables such as national energy and environmental policies and public-private partnerships [Error! Reference source not found.]. As we migrate from a carbon intensive fossil fuel-based freight transport system to a substantially/completely decarbonized freight transport system, several customer centric challenges need to be addressed. As compared to BEV or H<sub>2</sub> powertrains, fossil fuel-based powertrains provide mission flexibility, and high uptime at a relatively low total cost of ownership (TCO). While the incumbent carbon intensive powertrains suffer from poor

efficiency and are not sustainable to support Global Climate Change initiatives in transportation decarbonization, techno-economic challenges continue to create complex barriers to the large-scale displacement of these with highly electrified powertrains architectures [13,14,15]. Migration towards sustainable zero emission power in commercial vehicles with steady long-term adoption rates is dependent on both vehicle and infrastructure solutions that are well aligned with commercial vehicle end-user market needs. Their priorities are centered on: Availability (i.e. solutions are ready when it matters), Affordability (i.e. favorable economics), Efficiency (i.e. lower operational expenditure), Productivity (i.e. ability to get the job done), and Sustainability (i.e. emissions or CO<sub>2</sub> footprint/TCO/system-of-system capabilities). With fuel cell vehicles being an attractive option for the replacement of diesel-powered trucks, the refueling infrastructure along interstate highways demands a level of urgency to meet regulatory deadlines. For a sustainable freight transportation ecosystem, the supporting fueling infrastructure and the associated vehicle powertrains making use of hydrogen fuel will need to be optimized [16,17,Error! Reference source not found.].

Current refueling infrastructure (Figure 1) allows for diesel fuel to be transported, with relative ease, to various refueling locations including “behind the fence” locations such as distribution centers and port authorities, public refueling stations, and other shipping origins and destinations. The varying locations for a vehicle to refuel allows for optimal refueling strategies on the vehicular level, with flexibility for refueling options when weather and traffic adversely affect fuel economy.

Current infrastructure requirements literature is based on the needs to reduce GHG emissions and meet regulatory targets between 2030 and 2040 and the expected adoption rate of alternative fuel vehicles such as compressed and liquid natural gas, hydrogen FCEV, BEV and others with the main near-term focus being BEVs. The European Automobile Manufacturer’s Association estimates there will need to be approximately 30,000 500kW public chargers required by 2030 and 1,000 hydrogen refueling stations by 2030 [Error! Reference source not found.]. The International Council on Clean Transportation suggests that only 220 stations providing 4,800 kg of hydrogen a day will be required in the US, with that number rising to nearly 7,000 stations by 2050 [0]. Of note it is suggested that only 12% of heavy trucks on the road will be FCEV by 2050 with the remaining being a combination of BEV and ICE.

The first paper in this series explored the freight traffic demand and described methods of generating freight volumes and vehicle weights using the Freight Analysis Framework (FAF), Travel Monitoring Analysis System (TMAS), and other data sources to determine demand for hydrogen along I-75 [18]. The second paper in this series explored the cost of installing hydrogen refueling infrastructure and the impact demand have on total system cost as well as the impact on refueling time for commercial trucks [22]. In this paper, the third in the series, introduces the OR-AGENT (Optimal Regional Architecture Generation for Electrified National Transportation) tool developed at the Oak Ridge National Laboratory (ORNL), which has been used to optimize the hydrogen refueling infrastructure requirements on the I-75 corridor for HD FCEVs.

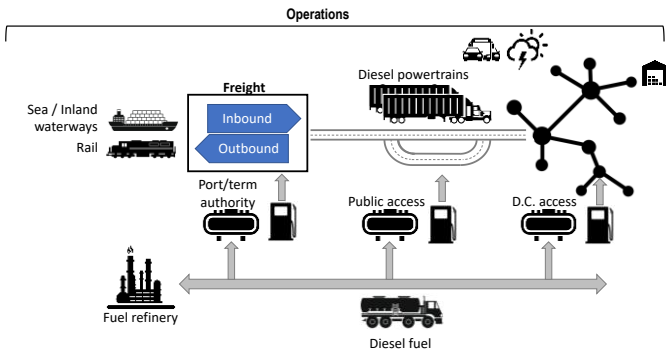


Figure 1. Diagram showing typical diesel refueling infrastructure

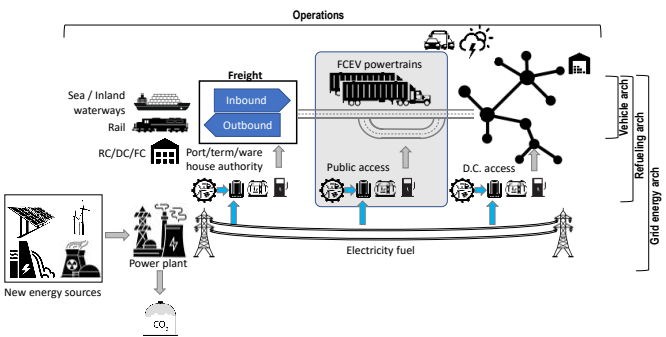


Figure 2. Complete architecture for FCEV with highlighted section indicating OR-AGENT focus for this paper

OR-AGENT is the evolution of the previous ORNL developed infrastructure planning tool, REVISE-II [23] that explored the location of electric chargers for battery electric vehicles. In the new OR-AGENT framework, a systematic multi-layered approach to on-highway freight transportation energy infrastructure is developed. The long-term objective of the tool is to provide an optimal zero emission vehicle powertrain and energy infrastructure architecture recommendation, that is regional specific, and accurately represents real world scenarios including freight movement, energy infrastructure, operational characteristics, and local constraints. This framework will assimilate the commercial vehicle first, middle, and last mile operations data including vehicle O-D weight and volume, the vehicle powertrain architecture options, supporting energy infrastructure components (both behind the fence and public access dispensing, storage, and DER), the electric grid energy production assets, regional constraints, and operating environment factors. It then uses advanced genetic algorithms to meet the objectives. Figure 2 shows the architecture considerations for OR-AGENT. The initial first phase construct (Figure 3 and topic of this paper) will incorporate various external data sets from powertrain simulations, existing infrastructure, and other sources to generate a realistic representation of the public access refueling requirements for HD FCEVs traveling on the I-75 freight corridor network. This will focus on the public refueling infrastructure typically found at travel centers and truck stops and makes assumptions that a vehicle can only fill up at these locations, as discussed later. Considerations into traffic, weather, grid impact and hydrogen generation are not considering in this first phase model.

The OR-AGENT model in this study will provide decisions on:

- Where should a refueling station be located to meet hydrogen demand?
- What is the hydrogen storage need at each station?
- How many dispensers should a refueling station have to meet hydrogen demand?

- What type of dispenser technology provides the lowest cost option while still meeting demand?

Previously studies have explored the optimization of refueling locations for various vehicle types including both passenger and commercial vehicles [24]. These studies have also explored the requirements for fuel transportation to refueling locations and various use cases for the specific refueling station using different mathematical models to determine origin-destination pairs and distance traveled of vehicles. The reoccurring assumption in these previous studies is that a vehicle has a finite driving distance absent of road grade or vehicle parameters. In our study, simulated vehicle dynamics will be incorporated to provide a realistic representation of driving range and refueling requirements.

Research on infrastructure needs revolve around

This paper will discuss the current data requirements for the model and how the data is generated. Secondly, the methods and steps required to incorporate the data and form a result. Lastly, a sample result will be discussed with a discussion of the conclusions and future opportunities.

## Model data inputs

Information from multiple data sources including Federal databases, simulations and other models have been combined to create an infrastructure optimization strategy for electrified transportation (Figure 3).

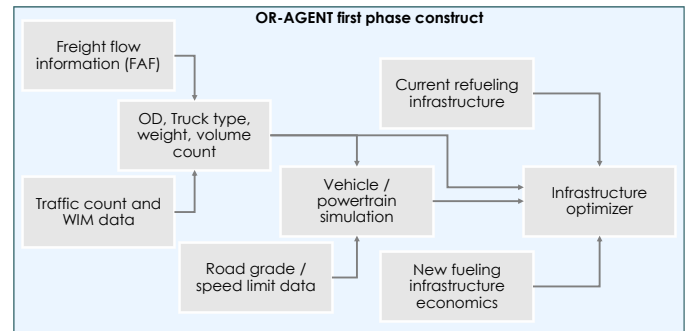


Figure 3. Data sources and structure of OR-AGENT for optimization of hydrogen refueling stations for commercial vehicles

The following data flows will be discussed in this section:

- **Freight Flow Information** – How freight moves along a route defined by an origin and destination
- **Traffic and Weight Data** – Distribution of heavy truck traffic along major corridors and the vehicle class and weight
- **Road grade and speed limit data** – Elevation/grade and speed limit along major road corridors
- **Vehicle & Power Train Simulation** – Simulation of vehicle and powertrain dynamics to determine fuel economy for segments along the given route
- **Current Refueling Infrastructure** – Location and demand distribution of potential refueling locations
- **New Infrastructure Economics** – Capital cost of new infrastructure deployment at a refueling station
- **Infrastructure Optimization** – Cost optimization for refueling locations based on the previous data inputs

### A. Freight Flow Information

FAF highway network was utilized for truck routing purposes [25]. To speed up truck routing, a network simplification process was first introduced to consolidate the network and to reduce the number of total highway links without losing information. In the process, for any two

adjacent links  $L_{a,b}$ ,  $L_{b,c}$ , if (i) no additional truck links are connected to the junction of the two links, denoted by node  $j$ , and (ii) the two links have the same speed limit, then the two adjacent links can be consolidated into one link connecting node  $a$  and  $c$ :  $L_{a,c}$ . A simple network example is shown in Figure 4(a). Green dots are the vertices of each road link before simplification while red circles represent the vertices after simplification. The speed limit of each link is marked in the figure. In the example,  $L_{a,c}$  and  $L_{c,e}$  cannot be consolidated because there is another link  $L_{c,d}$  that connect to node  $c$ .  $L_{c,d}$  and  $L_{d,e}$  cannot be consolidated because the two links have different speed limits.  $L_{a,b}$  and  $L_{b,c}$ , on the other hand, can be merged into one link  $L_{a,c}$  given both conditions are satisfied. Figure 4(b) shows a portion of the simplified FAF4 network. Similarly, green dots are the vertices of each road link in the FAF4 network. Red circles represent the vertices after simplification.

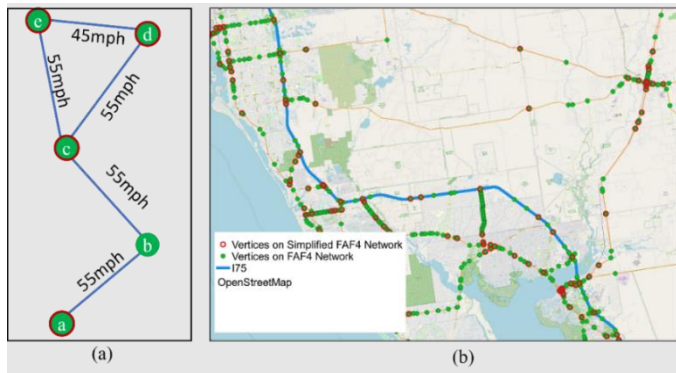


Figure 4. (a) Network simplification example, (b) FAF4 network vertices vs simplified FAF4 network vertices

**Truck routing:** It was assumed that all trucks will choose the shortest path between Origin (O) and Destination (D). There is a total of 132 origin FAF zones and 132 destination FAF zones in the FAF4 network. All truck movements were assumed to start from the centroid of the origin region and end at the centroid of the destination region. The same assumptions were adopted in previous studies [26]. The shortest path from 132 origin zones to 132 destination zones was obtained. All paths that traverse the I-75 corridor were then identified. Figure 5 shows an example of the resulting shortest path from the Detroit-Warren-Ann Arbor area to the Birmingham-Hoover-Talladega area. The shortest path (green lines) uses the I-75 corridor (black lines) from node E1 to node E2.

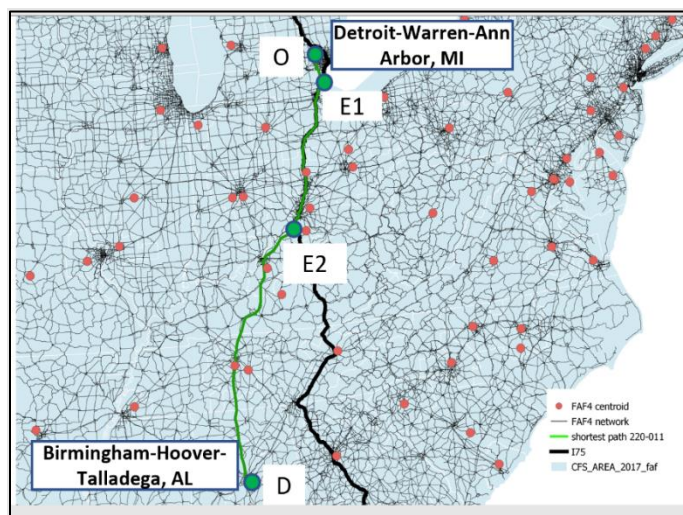


Figure 5. Shortest path from Detroit-Warren-Ann Arbor area to Birmingham-Hoover-Talladega area

Based on the routing results, each route from Origin to Destination is divided into three segments: (i) the segment from a FAF origin to the I-75 corridor entrance (e.g., O to E1 in Figure 5); (ii) The segment from the I-75 corridor entrance to the I-75 corridor exit (e.g., E1 to E2 in Figure 5); and (iii) the segment from the I-75 corridor exit to a destination (e.g., E2 to D in Figure 5). Note that a truck may leave the I-75 corridor for a bypass and reenter the same corridor again before reaching the destination. In these cases, there are more than three segments. The resulting O-D, and routed distance for each segment are the primary input data for truck hydrogen fuel consumption simulation.

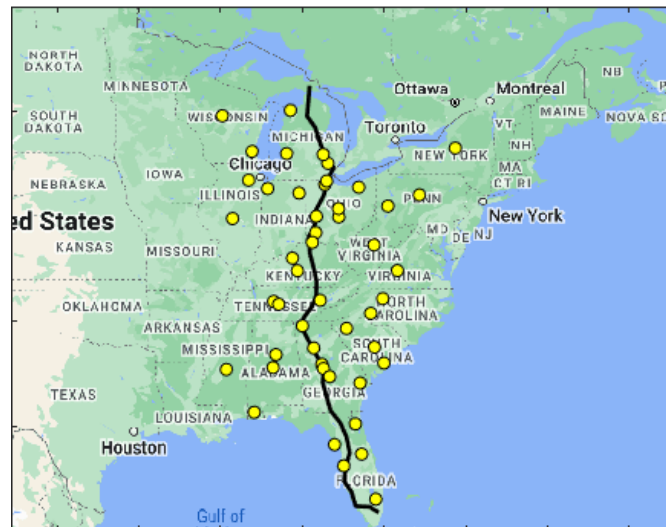


Figure 6. Location of Origin and Destinations considered for Heavy Truck travel along I-75

The daily average flow of heavy truck freight from the Freight Analysis Framework (FAF) was determined using the procedure described by Uddin [18]. Using the FAF network centroids for origin and destination, a routed distance to I-75 was calculated to determine how far a heavy truck would need to travel before reaching I-75. For the purposes of this study, only origin and destinations within 500 miles of I-75 were considered to ensure that the vehicle would be able to reach a refueling station before running out of fuel. The maximum routed distance traveled off I-75 was 499.4 miles and the maximum distance traveled on I-75 was 717 miles. Figure 6 shows the candidate origins and destinations used for the I-75 infrastructure optimization.

In addition to the distance traveled from origin to I-75 and from I-75 to destination, the distance traveled on I-75 was also calculated. Figure 7 shows the total daily distribution for vehicle trip length with many of the vehicles having a daily trip length of less than 600 miles, which aligns well with Federal Motor Carrier Safety Administration (FMCSA) hours of service (HOS) regulations [27] allowing, in most cases, allowing a maximum of 11 hours of daily driving. Trips over 600 miles may be split over multiple days of travel.

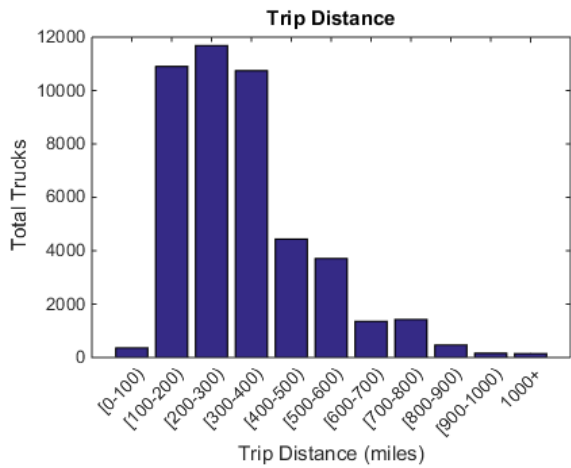


Figure 7. Distribution of Total Trip Length from Origin to Destination

**B. Traffic and Weight Data**

Vehicle class data for this study is represented by the FHWA notation which is based off vehicle configuration rather than weight (see Figure 8). Vehicle weight and class data for the previously generated O-D pathways was obtained from various data sources, such as the FAF Network tonnage, Travel Monitoring Analysis System (TMAS) weigh-in-motion (WIM) data [26]. Using distributions of weight for the vehicle class and location (example in Figure 9) a Gaussian Mixture Model was used to define three weights for each vehicle class (light, medium and heavy loaded). This info will be used to simulate vehicle fuel efficiency for a range of weights.

<b>Class 9</b> 5-Axle tractor semitrailer	
<b>Class 10</b> Six or more axle, single trailer	
<b>Class 11</b> Five or less axle, multi trailer	
<b>Class 12</b> Six axle, multi- trailer	
<b>Class 13</b> Seven or more axle, multi-trailer	

Figure 8. FHWA Heavy Vehicle Classification. Data taken from Ref. [28]

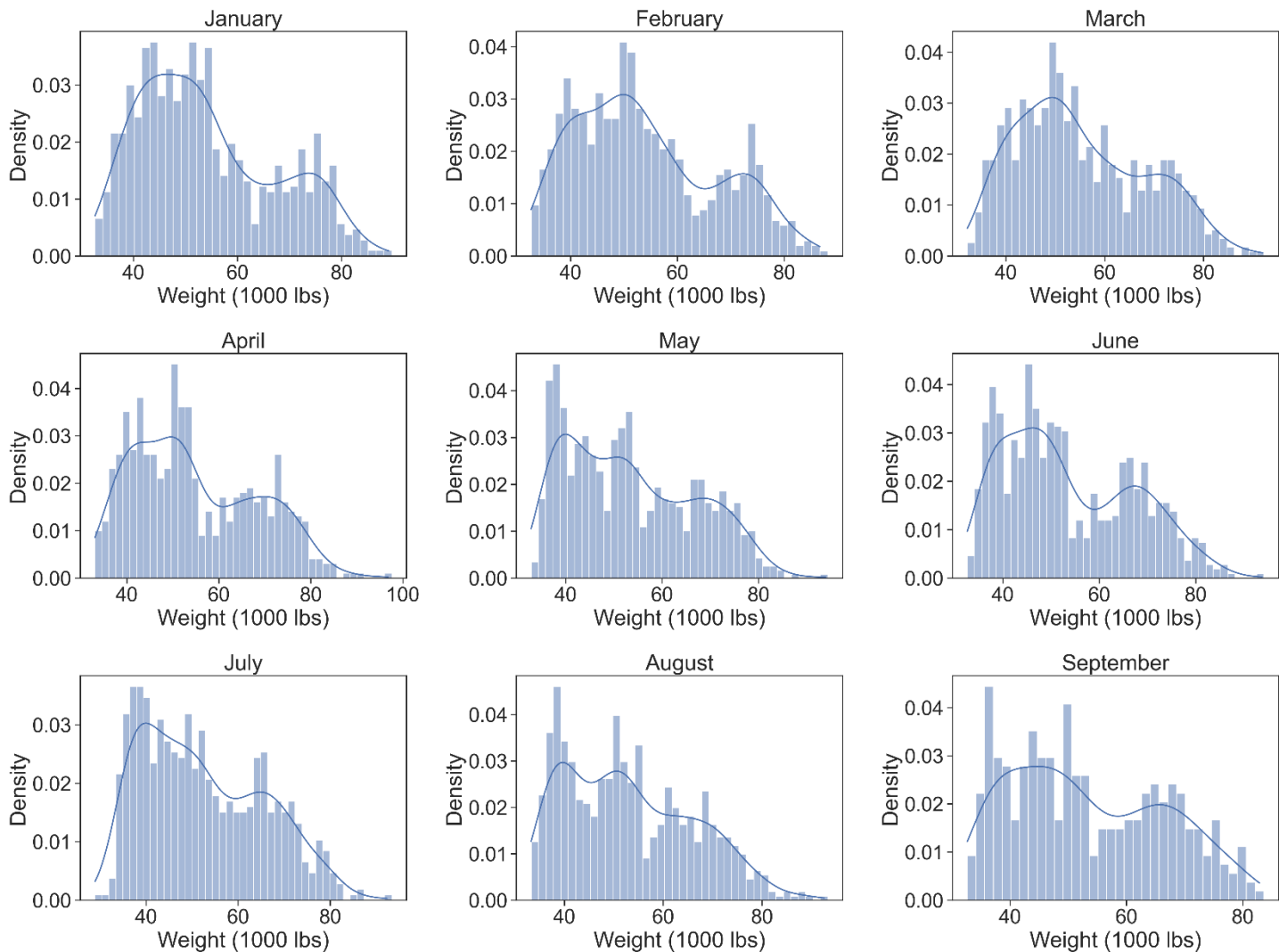


Figure 9. Sample Monthly Distribution of Weight Data at a Florida WIM station for Class 12 trucks

The monthly averaged weight distribution for Class 9-Class 13 heavy trucks is shown below in Figure 10, with 90% of the population for Class 9,11 and 12 being less than 60,000 lbs. and less than 85,000 lbs. for Class 10 and 11.

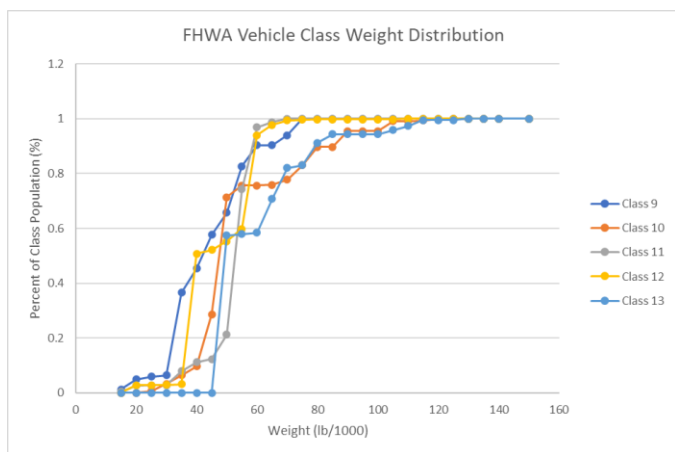


Figure 10. FHWA Vehicle Class Weight Distribution

The volume of traffic along the route defined by any origin and destination pair, was calculated from FAF Network data. The daily average truck volumes used in this research are modified by an

adoption rate described by the annual percentage of sale requirements of CARB [1,5] (Figure 11), with an upper limit of 45% of the total HD truck population. CARB's Advanced Clean Trucks (ACT) regulation requires manufacturers to sell increasing percentages of zero-emission trucks and is expected to further reduce the lifecycle emission of greenhouse gases and eliminate tailpipe emissions of air pollutants [1,5]. The ACT rule requires the sale of zero-emission or near zero-emission HD Trucks starting with the manufacturer-designated MY 2024 (see Figure 11). Sales requirements are defined separately for three vehicle groups: Class 2b-3 trucks and vans, Class 4-8 rigid trucks, and Class 7-8 tractor trucks [1,5]. The regulation is structured as a credit and deficit accounting system. A manufacturer accrues deficits based on the total volume of on-road HD truck sales within California in a given model year. These deficits must be offset with credits generated by the sale of zero- or near zero-emission vehicles (ZEVs/NZEVs) [1,5]. This adoption rate value was used to modify the daily truck volume, linearly, to determine the total amount of trucks that would be using hydrogen as percentage of the total population of trucks on I-75.

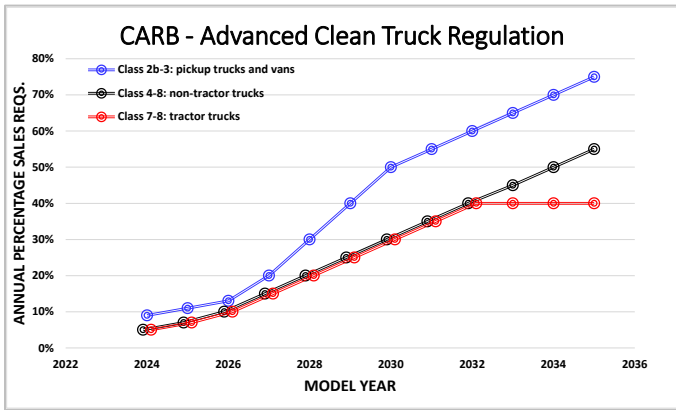
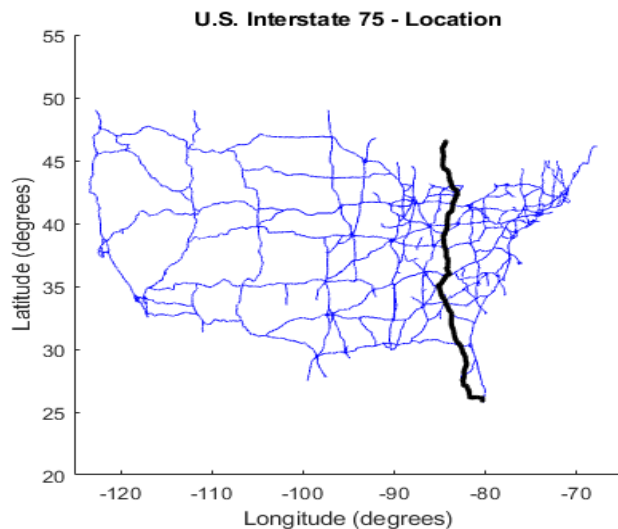


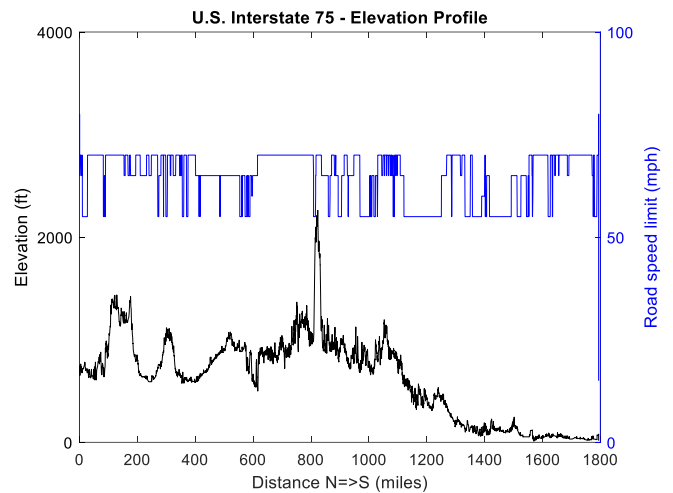
Figure 11. Adoption Rate of Vehicles by model year. Data taken from Ref. [2]

### C. Road grade and speed limit data

Road grade and vehicle road speed data are critical to assess the fuel consumption, and consequently, the refueling requirements along the I-75 corridor. Several data sources are combined to characterize this roadway for vehicle operations. Specifically, the Freight Analysis Framework 4 database is used to identify the GPS latitude and longitude coordinates of the I-75 corridor. All road elevation (grade) and speed limits are extracted from a higher accuracy, Nokia HERE database [29] at each reference GPS latitude and longitude coordinate. This process is used to leverage the preprocessing conducted by the FAF4 tool on GPS latitude and longitude coordinates associated with specific road names. In parallel, commercial tools such as the Nokia HERE database provide high accuracy assessments of elevation and road speed limits for a given GPS latitude and longitude coordinate. For this phase of the OR-AGENT framework, road speed limits are used as the vehicle speed targets (see Figure 12). Future manifestations of this approach will also leverage the actual road traffic flow rates at a given location, time, and date, to obtain a more representative real-world operating state for the vehicles. This will provide a real-world assessment of traffic and weather conditions.



(a) I-75 corridor (black) indicated among the entire U.S. interstate road system (blue)

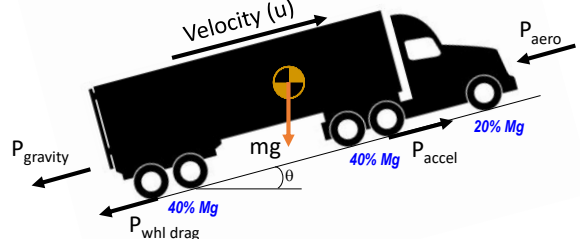


(b) I-75 elevation and road speed limits

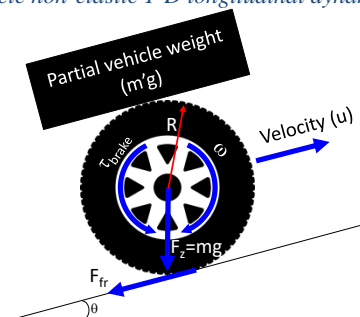
Figure 12. Characterizing the road grade and speed limits along I-75. Data taken from Ref. [25,29]

### D. Vehicle & Powertrain Simulation

Fuel economy for heavy trucks was calculated using a 1-D FCEV powertrain vehicle model as described by [16] with a range of fuel cell sizes to represent different vehicle configurations (Figure 14). The following equations from Sujan are the basis for the power calculations used for fuel economy in this paper.



(a) Vehicle non-elastic 1-D longitudinal dynamics model



(b) Wheel-tire-surface 1-D longitudinal model

Figure 13. Modeling the vehicle and road dynamics. Data taken from Ref. [16]

$$P_{\text{Propulsion}} = P_{\text{PwrSource}} = P_{\text{Aero}} + P_{\text{RR}} + P_{\text{Gravity}} + P_{\text{Accel}} + P_{\text{Loss}}$$

$$P_{\text{Aero}} = \left( \frac{\rho \cdot C_D \cdot u^2}{2} \right) u$$

$$P_{\text{RR}} = \left( C_{\text{rr-dyn}} (m \cdot g \cdot \cos\theta) u + C_{\text{rr-static}} (m \cdot g \cdot \cos\theta) \right) u$$

$$= (C_{\text{rr-dyn}} \cdot u + C_{\text{rr-static}}) \cdot (m \cdot g \cdot \cos\theta) u$$

$$P_{\text{Gravity}} = (m \cdot g \cdot \sin\theta) u$$

$$P_{\text{Accel}} = P_{\text{Accel Veh}} + P_{\text{Accel Wheel}} + P_{\text{Accel FD}} + P_{\text{Accel Trans}} + P_{\text{Accel Eng}}$$

$$= (m \cdot a) \cdot u + (I_{\text{whl}} \cdot \dot{\omega}_{\text{whl}}) \cdot \omega_{\text{whl}}$$

$$+ (I_{\text{FD}} \cdot \dot{\omega}_{\text{FD}}) \cdot \omega_{\text{FD}}$$

$$+ (I_{\text{Trans}} \cdot \dot{\omega}_{\text{Trans}}) \cdot \omega_{\text{Trans}}$$

$$+ (I_{\text{eng}} \cdot \dot{\omega}_{\text{eng}}) \cdot \omega_{\text{eng}}$$

$$P_{\text{Loss}} = P_{\text{Loss FD}} + P_{\text{Loss Trans}} + P_{\text{Loss Eng}} + P_{\text{Friction Tire Brake Loss}}$$

$$= \mathfrak{F}(\omega_{\text{FD in}}, \tau_{\text{FD in}}) \cdot \omega_{\text{FD in}} + \mathfrak{F}(\omega_{\text{Trans in}}, \tau_{\text{Trans in}}) \cdot \omega_{\text{Trans in}}$$

$$+ \mathfrak{F}(\omega_{\text{eng out}}, \tau_{\text{eng out}}) \cdot \omega_{\text{eng out}} + F_{\text{Fr}}(\mu, \lambda, m') \cdot u \quad (1)$$

$$I \dot{\omega} = F_{\text{fr}} \cdot R - \tau_{\text{brake}} \quad (2)$$

$$F_{\text{fr}} = \mu \cdot F_Z \cdot \cos(\theta) = \mu \cdot m' g \cdot \cos(\theta) \quad (3)$$

$$\lambda = \frac{u - (\omega \times R)}{u} \quad (4)$$

To simplify optimization calculations, an average fuel economy was calculated for 34, approximately 50-mile, segments along I-75 (Figure 15) for Class 9-Class 12 vehicles with five weights each (Table 1).

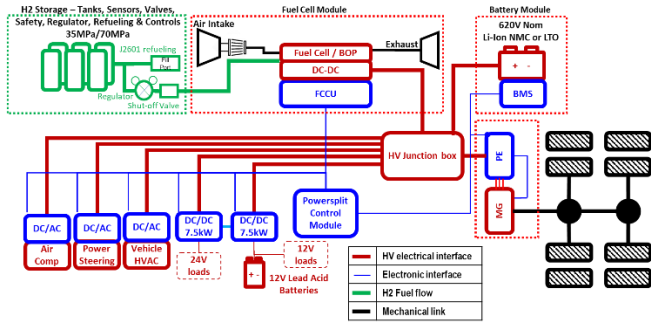


Figure 14. 1-D FCEV powertrain vehicle model

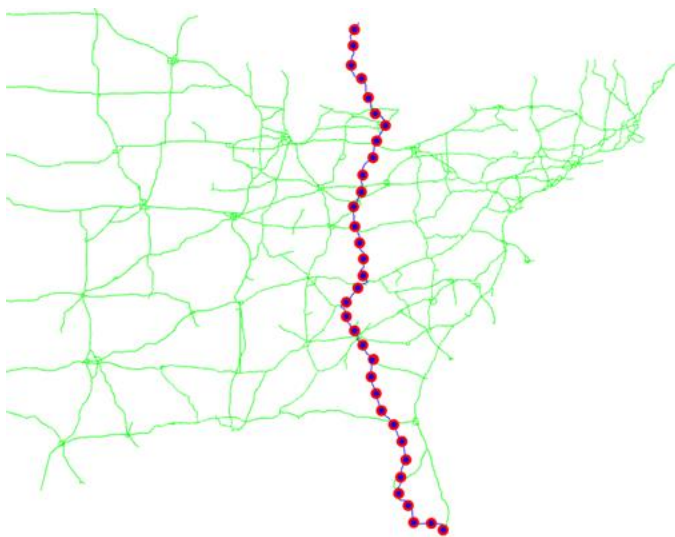


Figure 15. I-75 Segments for Fuel Economy Averages

Table 1. Vehicle Weights for Fuel Economy Simulation

FHWA Class	Vehicle Weight (lbs)					
	5th Percentile	25th Percentile	50th Percentile	75th Percentile	90th Percentile	95th Percentile
9	27,558	36,817	50,045	68,784	77,162	80,028
10	32,628	44,533	68,343	91,051	116,183	130,293
11	33,069	47,620	57,541	65,698	72,312	75,839
12	35,274	48,061	58,863	67,461	74,075	78,044
13	40,124	55,997	106,042	133,600	150,796	158,292

Figure 16 and Figure 17 capture the powertrain recommendations motivated by the CapEx and FuelEx minimization while also attempting to minimize product proliferation through inspection (valuable to both developers and end-users). These assessments with additional details were made previously [16]. In these tables energy capacity options of both a generic Li-ion NMC (Nickel Manganese Cobalt oxide – representing high energy battery chemistries) and LTO (Lithium Titanate – representing high power battery chemistries) batteries is provided [16, **Error! Reference source not found.**]. Characterizing the impact of battery chemistry is a complex problem and impacts the architectures associated with electrified powertrains including hybrid electric, battery electric, range extended electric, and fuel cell electric vehicles. Several studies have been and will continue to be conducted to explore battery characterization [16, **Error! Reference source not found.**, 30, 31, 32, 33, 34, 35]. Our previous studies have focused on a reduced order model on life, cost, power, and packaging, with the key results being used here [16]. The TCO and packaging studies conducted previously [16] marginally favor LTO over NMC battery chemistry architectures. It is important to state that significant development continues in the battery domain that will necessitate closer examination of the wider range of chemistry options that continue to be introduced (including gaps that currently exist in real long term durability assessments over real world operating scenarios). The range for both the fuel usage and the battery sizes is a result of the two different powersplit control algorithms—load following and energy minimization [16]. Figure 16 and Figure 17 summarize MY2020 and MY2030 Class 8 vehicle applications, but data has been assessed for the MY2040 specified vehicles. The focus of our work will use the architecture described by a vehicle architecture that represents a mature technology market [16]. For the purposes of this study, vehicles were assumed to have a 330-kW fuel cell (in addition to the long haul parameters listed in Figure 16 and Figure 17), and the resulting fuel economies, in kilograms of hydrogen consumed per mile, are shown for model year 2020 and 2030 tractors in Figure 18 and Figure 19, respectively.

<b>Short haul/dragage</b>		kW	225
		Kg	23-28
		kWh LTO NMC	28-52 91-245
<b>Daily Range: 150mi</b>		m <sup>2</sup> @ 7kg/s	1.6
		kW	285
		Kg	33-39
<b>Regional haul</b>		kWh LTO NMC	27-60 109-299
		m <sup>2</sup> @ 7kg/s	2.1
		kW	330
<b>Line haul</b>		Kg	89-95
		kWh LTO NMC	11-58 33-288
		m <sup>2</sup> @ 7kg/s	2.4
<b>Daily Range: 600mi</b>			

Figure 16. 2020 Architecture parameters
















 <p><b>Short haul/drayage</b></p> <p>Daily Range: 150mi</p>		<b>kW</b>	<b>225</b>
		<b>Kg</b>	<b>23-28</b>
		<b>kWh LTO NMC</b>	<b>27-51 89-240</b>
		<b>m² @ 7kg/s</b>	<b>1.6</b>
		<b>kW</b>	<b>285</b>
 <p><b>Regional haul</b></p> <p>Daily Range: 250mi</p>		<b>Kg</b>	<b>30-35</b>
		<b>kWh LTO NMC</b>	<b>25-58 106-292</b>
		<b>m² @ 7kg/s</b>	<b>2.1</b>
		<b>kW</b>	<b>330</b>
		<b>Kg</b>	<b>74-80</b>
 <p><b>Line haul</b></p> <p>Daily Range: 600mi</p>		<b>kWh LTO NMC</b>	<b>11-56 32-281</b>
		<b>m² @ 7kg/s</b>	<b>2.4</b>

Figure 17. 2030 Architecture parameters

	Class 9					Class 10					Class 11					Class 12					Class 13									
	27,558 lb	36,817 lb	50,045 lb	68,784 lb	77,162 lb	80,028 lb	32,628 lb	44,533 lb	68,343 lb	91,051 lb	116,183 lb	130,293 lb	33,069 lb	47,620 lb	57,541 lb	65,698 lb	72,312 lb	75,839 lb	35,274 lb	48,061 lb	58,863 lb	67,461 lb	74,075 lb	78,044 lb	40,124 lb	55,997 lb	106,042 lb	133,600 lb	150,796 lb	158,292 lb
1	10.39	9.38	8.52	7.28	6.71	6.65	9.80	8.80	7.24	6.21	5.25	4.94	8.67	7.63	7.02	6.69	6.45	6.22	8.05	7.30	6.78	6.46	6.10	6.01	7.51	6.70	4.95	4.36	4.06	3.97
2	8.79	8.15	7.28	6.50	6.16	6.05	8.31	7.63	6.51	5.67	5.04	4.65	7.20	6.57	6.15	5.84	5.64	5.59	6.88	6.28	5.95	5.64	5.45	5.29	6.32	5.79	4.52	4.06	3.75	3.67
3	8.09	8.06	7.30	6.41	6.11	5.96	8.26	7.61	6.38	5.65	5.00	4.70	7.18	6.51	6.12	5.82	5.66	5.56	6.79	6.26	5.89	5.59	5.45	5.36	6.32	5.71	4.59	4.09	3.93	3.81
4	8.77	8.16	7.33	6.46	6.12	6.00	8.44	7.67	6.47	5.66	5.02	4.78	7.29	6.61	6.12	5.87	5.71	5.58	6.82	6.27	5.97	5.63	5.42	5.32	6.39	5.80	4.57	4.05	3.87	3.71
5	9.18	8.59	7.70	6.79	6.39	6.33	8.87	8.07	6.78	5.85	5.20	4.77	7.61	6.85	6.44	6.16	5.90	5.78	7.22	6.59	6.14	5.87	5.62	5.54	6.68	6.06	4.61	3.96	3.70	3.56
6	8.78	8.16	7.45	6.49	6.16	6.06	8.40	7.69	6.53	5.69	4.96	4.63	7.28	6.55	6.22	5.89	5.70	5.58	6.85	6.31	5.94	5.64	5.44	5.26	6.38	5.75	4.44	3.88	3.56	3.51
7	9.00	8.39	7.48	6.55	6.29	6.10	8.56	7.80	6.53	5.69	5.05	4.67	7.40	6.79	6.38	6.00	5.77	5.72	7.05	6.50	6.11	5.74	5.52	5.41	6.53	5.94	4.61	4.06	3.78	3.67
8	9.10	8.40	7.51	6.60	6.26	6.07	8.63	7.76	6.59	5.70	4.94	4.64	7.52	6.72	6.26	6.00	5.69	5.59	7.06	6.46	6.03	5.70	5.52	5.40	6.60	5.89	4.48	3.89	3.59	3.52
9	9.60	8.85	7.96	6.95	6.59	6.45	9.22	8.35	6.92	6.02	5.22	4.86	8.06	7.16	6.72	6.36	6.07	5.98	7.52	6.87	6.43	6.10	5.85	5.69	7.04	6.29	4.77	4.14	3.80	3.68
10	9.67	8.92	8.19	7.10	6.68	6.56	9.32	8.45	7.08	6.14	5.30	4.93	7.99	7.23	6.79	6.42	6.12	6.08	7.60	6.93	6.46	6.10	5.90	5.81	7.09	6.34	4.82	4.21	3.88	3.76
11	9.88	9.17	8.22	7.15	6.70	6.52	9.52	8.54	7.07	6.11	5.33	4.92	8.18	7.37	6.84	6.46	6.23	6.11	7.78	7.07	6.61	6.23	5.98	5.82	7.28	6.45	4.93	4.28	3.96	3.81
12	9.73	8.96	7.95	6.88	6.47	6.33	9.27	8.41	6.89	5.91	5.17	4.84	8.16	7.14	6.67	6.35	6.11	5.96	7.69	6.95	6.44	6.13	5.90	5.69	7.15	6.38	4.89	4.39	4.11	4.02
13	8.44	7.92	7.07	6.25	5.93	5.83	8.05	7.35	6.28	5.52	4.91	4.57	6.93	6.34	5.93	5.69	5.47	5.37	6.55	6.05	5.74	5.45	5.25	5.18	6.11	5.62	4.44	3.99	3.74	3.71
14	8.27	7.74	7.00	6.15	5.81	5.75	8.06	7.24	6.16	5.44	4.86	4.55	6.86	6.25	5.87	5.63	5.40	5.32	6.50	5.99	5.68	5.41	5.21	5.10	6.04	5.57	4.41	3.97	3.72	3.62
15	8.35	7.70	7.01	6.33	6.11	6.07	7.89	7.31	6.33	5.74	5.12	4.83	6.87	6.33	6.05	5.82	5.66	5.59	6.50	6.14	5.84	5.60	5.44	5.42	6.18	5.73	4.72	4.33	4.17	4.01
16	8.69	8.02	7.21	6.66	6.47	6.47	8.34	7.48	6.64	6.10	5.59	5.27	7.16	6.60	6.32	6.17	6.01	6.00	6.86	6.41	6.16	5.95	5.81	5.86	6.47	6.01	5.27	4.79	4.60	4.52
17	9.60	8.75	7.73	6.67	6.41	6.31	9.01	8.07	6.67	5.96	5.35	5.04	8.02	7.01	6.56	6.26	6.01	5.90	7.46	6.82	6.29	6.02	5.85	5.73	6.98	6.27	4.99	4.54	4.33	4.25
18	9.51	8.81	7.84	6.70	6.41	6.27	9.17	8.15	6.79	5.83	5.12	4.73	7.89	7.05	6.55	6.23	5.94	5.84	7.44	6.76	6.24	5.94	5.75	5.60	6.98	6.20	4.69	4.15	3.89	3.79
19	10.62	9.63	8.52	7.38	7.02	6.84	10.02	8.98	7.37	6.40	5.61	5.26	8.75	7.82	7.24	6.95	6.59	6.51	8.29	7.55	6.94	6.65	6.40	6.29	7.77	6.90	5.37	4.82	4.47	4.38
20	9.34	8.55	7.63	6.71	6.37	6.25	8.93	7.97	6.70	5.85	5.24	4.95	7.60	6.89	6.47	6.16	5.94	5.90	7.27	6.65	6.26	5.89	5.68	5.59	6.82	6.16	4.87	4.41	4.14	4.06
21	8.69	8.02	7.14	6.20	5.93	5.73	8.39	7.46	6.20	5.42	4.77	4.44	7.25	6.46	6.05	5.78	5.57	5.44	6.84	6.24	5.80	5.52	5.32	5.24	6.38	5.77	4.44	3.96	3.74	3.57
22	11.82	10.69	9.30	7.96	7.46	7.30	11.16	9.87	7.94	6.81	5.94	5.46	9.81	8.58	7.85	7.42	7.04	6.88	9.27	8.30	7.53	7.16	6.76	6.73	8.66	7.58	5.59	4.97	4.61	4.52
23	12.55	11.28	9.79	8.32	7.90	7.66	11.74	10.49	8.42	7.10	6.06	5.65	10.56	9.08	8.35	7.87	7.46	7.33	9.93	8.74	8.04	7.49	7.19	6.92	9.17	7.97	5.79	5.07	4.71	4.54
24	11.93	10.96	9.70	8.37	7.80	7.61	11.42	10.14	8.30	7.07	6.06	5.63	9.90	8.89	8.11	7.74	7.22	7.14	9.36	8.55	7.85	7.34	7.07	6.87	8.75	7.82	5.72	4.92	4.55	4.41
25	8.75	8.09	7.29	6.48	6.09	6.03	8.30	7.57	6.48	5.63	4.90	4.57	7.21	6.60	6.18	5.86	5.62	5.47	6.85	6.23	5.86	5.55	5.37	5.22	6.30	5.69	4.38	3.85	3.69	3.59
26	10.20	9.36	8.34	7.24	6.86	6.61	9.75	8.77	7.28	6.26	5.36	4.98	8.44	7.54	7.05	6.67	6.41	6.20	8.05	7.21	6.81	6.33	6.14	5.97	7.37	6.68	5.01	4.35	4.02	3.86
27	11.43	10.34	9.22	7.81	7.31	7.21	10.94	9.61	7.73	6.59	5.72	5.32	9.49	8.40	7.64	7.19	6.90	6.75	8.92	7.99	7.40	6.93	6.67	6.42	8.29	7.41	5.38	4.72	4.38	4.26
28	12.65	11.67	10.23	8.68	8.22	7.99	12.13	10.74	8.78	7.29	6.29	5.79	10.70	9.40	8.59	8.14	7.76	7.63	9.96	9.02	8.27	7.79	7.40	7.16	9.31	8.21	5.97	5.15	4.73	4.64
29	11.13	10.16	8.96	7.82	7.36	7.17	10.65	9.53	7.81	6.64	5.75	5.36	9.31	8.30	7.69	7.19	6.90	6.68	8.81	7.97	7.32	6.85	6.63	6.46	8.16	7.21	5.36	4.69	4.34	4.21
30	9.35	8.61	7.72	6.70	6.37	6.17	8.91	7.97	6.74	5.83	5.00	4.63	7.71	6.91	6.46	6.10	5.89	5.73	7.27	6.65	6.17	5.89	5.56	5.54	6.74	6.09	4.56	3.95	3.64	3.48
31	9.51	8.22	7.52	6.56	6.16	6.07	8.56	7.68	6.61	5.71	4.92	4.58	7.36	6.67	6.22	5.93	5.71	5.56	6.91	6.32	5.98	5.66	5.45	5.30	6.42	5.86	4.44	3.88	3.54	3.42
32	8.56	7.84	7.14	6.42	5.96	5.90	8.19	7.50	6.35	5.54	4.84	4.48	7.09	6.41	6.02	5.70	5.49	5.37	6.69	6.15	5.77	5.45	5.24	5.21	6.22	5.66	4.26	3.70	3.40	3.25
33	8.53	7.89	7.17	6.38	6.05	5.95	8.12	7.48	6.44	5.59	4.86	4.51	7.03	6.41	6.04	5.79	5.53	5.45	6.65	6.17	5.75	5.48	5.27	5.23	6.21	5.69	4.28	3.72	3.39	3.22
34	8.91	8.30	7.55	6.60	6.24	6.14	8.71	7.78	6.57	5.69	5.01	4.67	7.45	6.73	6.32	6.01	5.79	5.63	7.05	6.50	6.00	5.68	5.50	5.37	6.57	5.90	4.47	3.84	3.55	3.43

Figure 18. MY 2020 direction averaged fuel economies for 330 kW FC Vehicle (kg/mile)

	Class 9					Class 10					Class 11					Class 12					Class 13									
	27,558 lb	36,817 lb	50,045 lb	68,784 lb	77,162 lb	80,028 lb	32,628 lb	44,533 lb	68,343 lb	91,051 lb	116,183 lb	130,293 lb	33,069 lb	47,620 lb	57,541 lb	65,698 lb	72,312 lb	75,839 lb	35,274 lb	48,061 lb	58,863 lb	67,461 lb	74,075 lb	78,044 lb	40,124 lb	55,997 lb	106,042 lb	133,600 lb	150,796 lb	158,292 lb
1	12.51	11.42	10.13	8.68	8.17	7.95	11.77	10.45	8.74	7.39	6.29	5.85	10.43	9.14	8.41	7.81	7.57	7.46	9.71	8.76	7.93	7.62	7.22	7.09	9.04	7.94	5.81	5.13	4.77	4.62
2	10.71	9.98	8.93	7.78	7.45	7.40	10.37	9.38	7.93	6.88	6.06	5.64	8.83	7.82	7.37	7.01	6.84	6.70	8.13	7.54	7.11	6.75	6.49	6.40	7.62	6.83	5.40	4.83	4.52	4.35
3																														



weight for each FHWA vehicle class using a 330-kW fuel cell. As one would expect, the fuel economy decreases as the vehicle becomes larger (more trailers and axles) and heavier. Due to the amount of different origin to destination paths for the current research, fuel economies for the trip length from an origin to I-75 and I-75 to the origin were not explicitly calculated. To get a representative fuel economy for each vehicle class and weight range, the average of the 34 segments on I-75 were used as the fuel economy for those segments of road not on I-75. This is an area for future research and development as it increases simulation and calculation time.

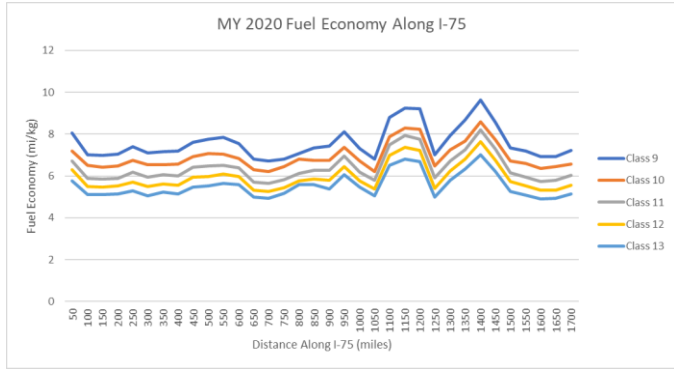


Figure 20. 90th percentile GCVW fuel economy for segments along I-75 for MY2020 vehicles with 330-kW FC

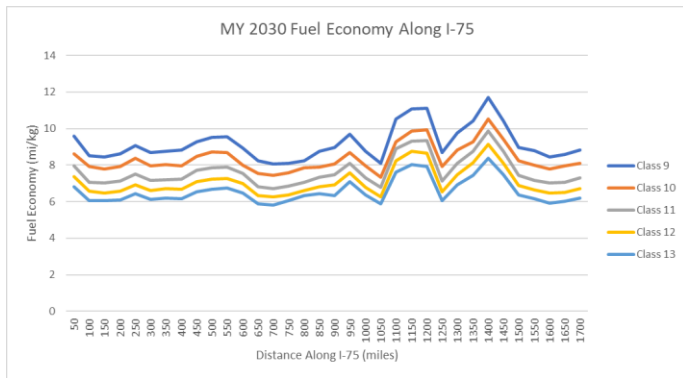


Figure 21. 90th percentile GCVW fuel economy for segments along I-75 for MY2030 vehicles with 330-kW FC

### E. Current Refueling Infrastructure

The current refueling infrastructure is dominated by diesel stations along major interstate corridors and distribution centers. Freight typically originates from either a terminal (sea port, inland waterway port, rail terminal or air freight terminal) and is transported by truck to a distribution center, warehouse, factory, or other waypoint for further processing and transport. Much of the freight movement is performed by diesel trucks until a last mile portion of the system. Refueling can happen at various locations depending on the carrier operations: 1) at a private or access-controlled facility such as a port authority or

distribution center, or 2) at public access diesel stations. The fuel for these stations is typically transported by truck to each location from a central location, such as a pipeline. Figure 1 shows the typical refueling infrastructure for diesel trucks.

The goal of the current model framework is to identify, characterize, and use existing locations as candidate stations for refueling to represent where vehicles would typically refuel. While a new station may be readily identified and characterized by the process developed in this paper, for the purposes of this study it is assumed that the emerging hydrogen infrastructure will likely begin by phasing in hydrogen fuel storage/dispensing capabilities at established (brownfield) refueling sites as opposed to new (greenfield) sites. The location of current diesel refueling infrastructure was obtained using publicly available data from the Geotab Ignition [36] dashboard which uses anonymized customer data to provide data trends. Using this dashboard, the authors were able to filter the location data to determine where HD trucks refuel and at what time of day to determine potential refueling locations for hydrogen trucks. For the purposes of this study, only refueling stations located in a State along the I-75 corridor, with a minimum of 75% heavy truck traffic were considered (Figure 22). This filtering ensured that the refueling stations exported were major truck stops, where a heavy truck would likely refuel, rather than refueling stations that may have at least one diesel dispenser.

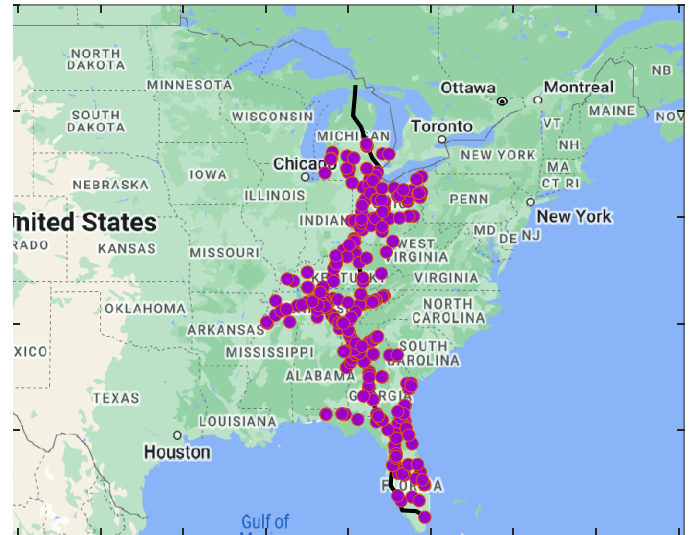


Figure 22. Location of Refueling Locations near the I-75 corridor from Geotab Ignition

Data elements exported from the Geotab Ignition dashboard include the latitude and longitude of the refueling station, the percentage of heavy truck traffic, and the hourly heavy truck demand. The hourly demand (Figure 23) was normalized to the total heavy truck population for the refueling station. While the Geotab data does not represent the entire population of tractors on the roadways, it is assumed that the hourly demand obtained is like that of the entire population for this study.

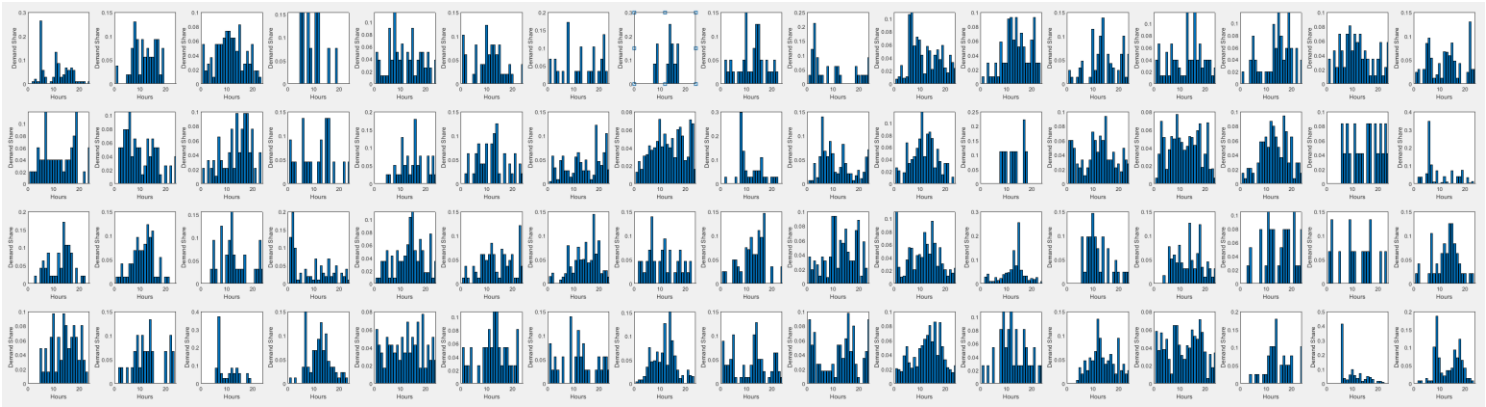


Figure 23. Distribution of station hourly demand for candidate stations. Each figure represents the demand for a single station along the I-75 corridor. While there are many more fueling stations along I-75, these 68 stations capture the commercial truck refueling stations.

**F. New Infrastructure Economics**

The capital cost of new infrastructure is critical to optimizing the location of potential refueling stations for heavy trucks. Using the methods defined by Liu [22] using the Heavy-Duty Refueling Station Analysis Model (HDRSAM) [37], capital cost was calculated as a function of daily demand (number of trucks), dispenser fill rate (technology), number of required dispensers, and the hourly demand for a given station. Figure 24 shows example costs calculated using the HDRSAM model.

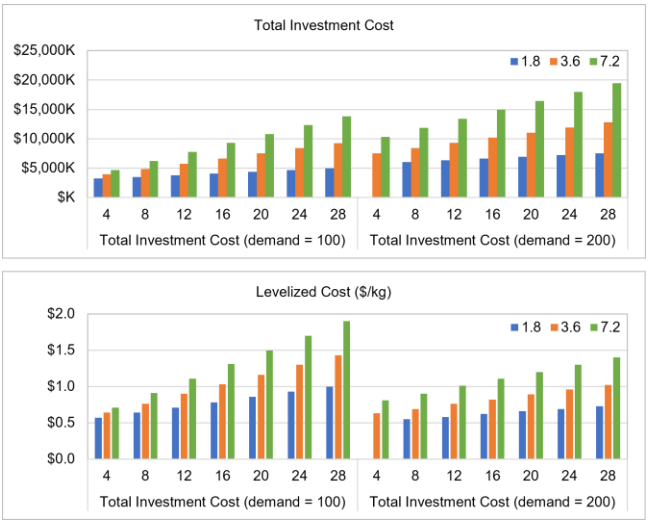


Figure 24. Total investment cost and Levelized cost by demand

To incorporate these results into a computational model, absent of the HDRSAM algorithms, and without calculating every single permutation vehicle demand, look up tables were generated for each of dispenser technology (e.g. 1.8, 3.6 and 7.2 kg/min dispensers). Individual values of demand, dispenser count, or truck volume that were not explicitly in the table were interpolated between known values to determine a reasonable cost for the station. Future work on the model will aim to incorporate a more direct cost function to accurately calculate the cost of a particular station.

**G. Infrastructure Optimization**

The optimization workflow for refueling location strategy is a computational model developed using the previously discussed inputs using the following steps:

- **Step 1:** Candidate station generation – Determine valid refueling locations based on distance from I-75
- **Step 2:** Route segment and volume generation – consolidate

routes that overlap to reduce computational time

- **Step 3:** Feasibility calculation – calculate the locations of refueling and determine how many trucks will stop daily and how much fuel will be required
- **Step 4:** Station Cost optimization – calculate the cost of a station meeting the minimum fueling and demand requirements prescribed in previous steps

**Step 1 – Candidate Station Generation**

To determine the location of stations along I-75, the distance each of the refueling stations obtained from the Geotab Ignition dashboard from I-75 was determined using a geohash representation. A geohash is a convenient way of representing latitude and longitude alpha numerically using a grid-based system [38]. A Geohash is a unique identifier of a specific region on the Earth. The basic idea is that the Earth is divided into regions of user-defined size and each region is assigned a unique identifier based on its latitude and longitude, which is called its Geohash—an alpha numeric string. This string or Geohash, will determine which of the predefined regions the point belongs to. Thus, points within close geographical proximity will have the same Geohash. The length of the geohash determines the accuracy to specific location (e.g. 7 characters creates an area of approximately 0.2 square kilometers and 10 characters is approximately an area 0.7 square meters). For this study 7 characters were used for the precision of accuracy and were considered to be a candidate location if the first 5 characters of the geohash matched a location on I-75 (24 square kilometer area or within about 6 miles of I-75). This precision was used because it is assumed that vehicles will be dispatched full of fuel and not require a refuel for many miles. These candidate stations (shown in Figure 25) represent the chromosomes in the genetic algorithm previously discussed.

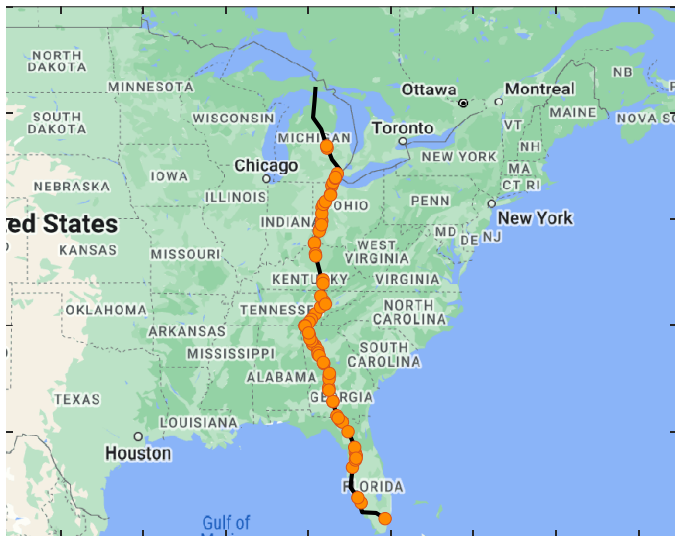


Figure 25. 68 Candidate station locations along I-75

For some scenarios (Figure 26), multiple refueling stations could be present at the same location (major junctions could have multiple truck stops). In this scenario, the stations were grouped into a single location with the demand averaged for the refueling stations and the maximum number of dispensers allowed to increase to 20 (maximum parameter) per station (i.e. 40 dispensers for a location with 2 stations).

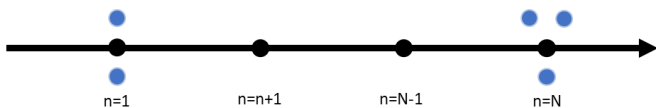


Figure 26. Diagram showing grouping of common candidate locations along I-75

The calculation of candidate stations is deterministic on the route chosen. For this study, since the focus was on I-75, the candidate stations were static for all iterations of the model unless parameters are changed to allow for stations to exist farther from I-75. The genetic algorithm will be discussed in later sections of this paper.

### Step 2 – Route Segment and Volume Generation

Identifying the segments along a route that vehicle will travel is required to calculate total distance traveled on a particular segment and the amount of fuel used on that segment. To accomplish this, every O-D pair is assigned an “entry” and “exit” point on I-75 to calculate both the distance traveled off I-75 and the distance traveled on I-75. For the distance traveled off I-75, the distance is simply a calculated routed distance. Similarly for distance traveled on I-75, the distance is a calculated routed distance, but additional node information is available. Thus, a list of locations that a vehicle will travel through on its trip is calculated.

To efficiently iterate through large lists of trips, and because it is known that many of these route’s overlap, common routes are grouped to calculate a total volume for the given segment of I-75.

### Step 3 – Feasibility Calculation

To determine the daily total trucks and the amount of fuel required, each unique route previously calculated is iterated through to determine the total number of each vehicle class that will stop at each refueling station and how many kilograms of hydrogen will be required.

To calculate fuel level during a trip, and the total fuel required by a

particular refueling station, each segment of road in an O-D pair is iterated over with the total amount of fuel required to traverse that segment being subtracted from the previous tank level. While iterating, if the total amount of fuel drops below a parameterized fuel level, it will fill up at the next location. Since it is assumed as part of this study that every vehicle starts the trip full, it is known exactly how much fuel will be required to top off the tank.

After each O-D pair is iterated through, the result is a total number of vehicles that will stop daily at a given station, and the total amount of fuel required daily. If a vehicle could not make the trip because it ran out of fuel due to a refueling station not existing on their route or simply not having a large enough tank to make the trip, it is considered infeasible. Each infeasible vehicle would essentially be a waste of capital for a company and another vehicle capable of making the trip would have to be used in its place, so a variable infeasibility cost is applied for each truck that cannot complete the trip.

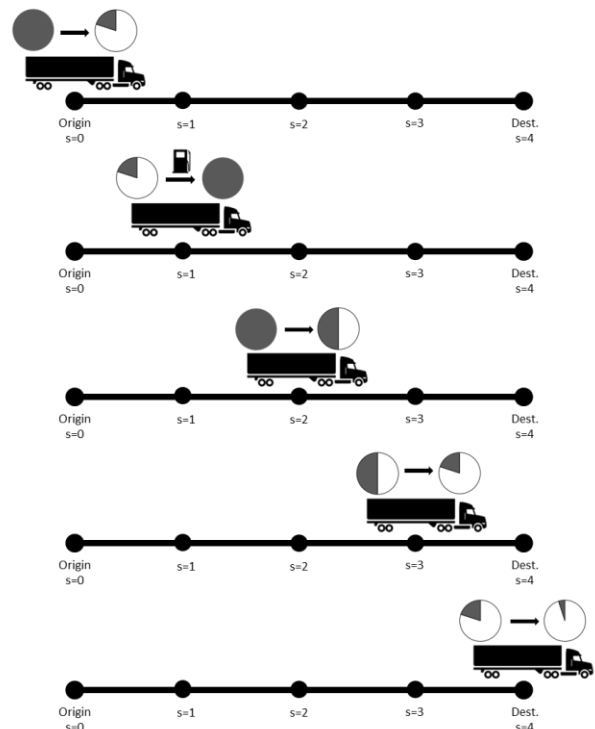


Figure 27. Refueling strategy for each O-D Pair

### Step 4 – Station Cost Optimization

There are stochastic operations in hourly demand share  $\alpha_t$  (% ,  $t \in \{1, \dots, T\}$ ) between stations in one area. Given the total daily fuel demand  $D$  (kg/day) for a station where the capacity is needed to be designed, the actual demand share could be any of the possible scenarios. With design refueling speed  $s$  (kg/hour) for single fuel dispenser, the problem is to determine the number of dispensers,  $Z$ , to be installed at the station to support the total fuel demand  $D$  considering potential delays to truck drivers. As installing dispensers is capital intense, one objective is to minimize  $Z$  to support the fueling demand. On the other hand, with fewer dispensers, delays are possible to occur when the demand temporally exceeds the supply. Another objective is the minimize the total delay which could be costly to the truck business. Therefore, there is a tradeoff between the infrastructure cost and the operational cost.

There are two simple, albeit limited, methods to determine  $Z$ . One is based on the average fuel demand. Given the number of operational hours  $T$  ( $T = 24$ ) in a day, the average hourly fuel demand is  $D/T$ .

Then based on the average fuel demand, it can be determined:

$$Z_{average} = \left\lceil \frac{D}{Ts} \right\rceil \quad (5)$$

However, such design ignores the stochasticity in operations with non-uniform distribution on  $\alpha_t$ . A station with this design cannot meet the peak  $\alpha_t$  and could cause significantly delay to drivers.

Another way is the design the capacity based on the maximum hourly rate, namely:

$$Z_{maximum} = \left\lceil \frac{D \cdot \sup(\alpha_t)}{s} \right\rceil \quad (6)$$

A station with this design will not have any delay to trucks in all periods but could incur significant capital cost to the station infrastructure.

A better way is to consider the hourly patterns in all scenarios and determine  $Z$  considering the cost tradeoff. A stochastic programming model is formulated and described here with the following objective function:

$$\text{Min } cZ + \sum_{\omega \in \Omega} \sum_{t \in \{1, \dots, T\}} \theta_{\omega} \frac{qN}{D} y_{t\omega} \quad (7)$$

Subject to the following constraints:

$$x_{t\omega} \leq sZ \quad (8)$$

$$x_{t\omega} = \alpha_{t\omega} D + y_{t-1, \omega} - y_{t\omega} \quad (9)$$

Table 2. Formulation Notation

Set	
$\Omega$	Indexed by $\omega$ , set of refueling demand pattern scenarios
Parameters	
$D$	Total daily fuel demand (kg)
$N$	Total daily number of trucks to refuel at the station
$s$	Design refueling speed (kg/hour) of the dispenser
$\alpha_{t\omega}$	Demand share (%) in time $t$ in scenario $\omega$
$c$	Daily capacity cost (\$/day) for a dispenser
$q$	Penalty cost on waiting and delay for refueling (\$/hour/truck)
$\theta_{\omega}$	Probability share (%) of the scenario $\omega$
Variable	
$Z$	Non-negative integer, the number of dispensers to be installed
$x_{t\omega}$	Actual fulfilled demand (kg) in time $t$ in scenario $\omega$
$y_{t\omega}$	Carryover remeet fuel demand for next hour ( $t + 1$ ) % $T$

### 1. Genetic algorithm (GA) overview

To solve the model optimally for the large number of permutations, a genetic algorithm was adapted from previous research [21] to determine which refueling stations need to be open and what type of refueling technology is present at that location. The total number of possible refueling scenarios is calculated using the one of following equations:

$$R_{fuel} = 1 + \sum_{n=1}^N T * (T + 1)^{n-1} \quad (10)$$

$$R_{fuel} = S^N \quad (11)$$

Where  $N$  is the number of candidate stations,  $T$  is the number of refueling technologies (e.g. 1.8 kg/min @ 350bar, 3.6 kg/min @ 350bar, 7.2 kg/min @ 350bar), and  $S$  is the number of station states (i.e., equal to  $T+1$ , where the additional state is the null state representing the lack of hydrogen infrastructure). For the current problem in this research, the total number of permutations would be  $4^{68}$  which would take a significant amount of calculation time for an exhaustive search for the optimal configuration.

Even though station capacity can be formulated as piecewise linear relationship, the mixed integer program is still hard to solve optimally. We developed a genetic algorithm based heuristic method [39] to solve the model. Generally, the genetic algorithm involves a pool of chromosomes. Each chromosome represents one candidate solution to the problem, and the fitness of each candidate solution is measured by the cost objective value. Between chromosomes, the one with a lower objective value indicates better fitness. The algorithm has an iterative process, during which chromosomes with bad fitness are more likely to be removed from the pool while chromosomes with good fitness have more chances to survive and give birth to a new child. The whole process mimics natural selection. It is generally observed that through multiple iterations the genetic algorithm can help find near optimal or relatively satisfactory solutions.

While the genetic algorithm served as a great estimation of the locations of fueling infrastructure for hydrogen FCEV, future iterations of the OR-AGENT tool will adapt dynamic programming to find a more global solution, at the cost of additional compute time and computational resources.

### 2. Implementation details

Two features are important to efficiently apply a genetic algorithm. One is the simplicity in coding the solution with chromosomes, and the other is to be able to easily determine fitness given the genetic information of one chromosome. However, both features are hard to maintain for the proposed model. First, as in Li et al.'s study [40], only two-dimension infrastructure related decision variables, i.e., where and when refueling stations are opened, are needed to be encoded in the chromosome. However, this task is more challenging for this study because the model requires another dimension on capacity-related decisions, i.e., how many dispensers per station. That creates challenges in coding all decision information in each chromosome. Second, as capacity is considered for each fueling, the heuristic approach to check path feasibility with infinity capacity [38] is not applicable to this study. Instead, mixed integer programming sub-models need to be solved, which makes it difficult to efficiently determine fitness for each chromosome generated in the solution process.

To tackle the two challenges in this complex model we made the following assumption to simplify the FCEV fueling behavior: If an O-D path at one stage is feasible and selected given fueling infrastructure deployment, refueling stations along the path will have sufficient dispensers to satisfy all O-D traffic demands along the path in the same time stage. This assumption is already inherently built into the proposed model, which considers only the feasibility of each O-D pair instead of each O-D trip. This assumption is reasonable to provide equity for all travel demand along each O-D pair.

This method simplifies the solution process for the model in the following ways. First, it will significantly simplify the determination of fitness of each chromosome with heuristic methods. Given the setting of refueling stations at each time stage encoded in each chromosome (where and when to open stations), the heuristic approach [38,39] can be used to efficiently check path feasibility of all O-D pairs. Following this assumption, we can determine the number of dispensers needed for each station to satisfy all refueling demand.

Finally, the fitness of the chromosome can be calculated using the objective function. Second, as suggested in the first benefit, the number of dispensers per station can be post-calculated. Therefore, only decisions on where and when refueling stations are opened need to be encoded in each chromosome. That simplifies the representation of each chromosome.

### 3. Settings of genetic algorithms

Based on the above properties and assumptions of the problem, we made the following settings to apply the genetic algorithm to solve the proposed model.

#### 3.1 Encoding of chromosome

As previously described, only decisions on where and when fueling stations are opened need to be encoded into each chromosome. Since each opened refueling station will remain open once it is in operation, only the time when the refueling station is first opened needs to be recorded. Therefore, we used a single dimension integer valued string to represent such information. Each digit entry along the chromosome string represents one specific candidate location. Then, the total length of the string is  $|N|$  (the number of candidate locations). Each digit can take non-negative integer values. When the digit takes a value of 0, it indicates no refueling station is opened at the location throughout the time horizon. When the digit takes a positive value of  $i$ , it indicates the type of dispenser technology at the opened station.

Consider the simple example chromosome string “01020” to demonstrate its meaning on refueling infrastructure planning decisions as follows:

- Five digits in the string indicate five candidate locations ( $|N|= 5$ ) for fueling stations
- No fueling station is opened at candidate locations 1, 3, and 5
- One fueling station is opened at candidate location 2 with 1.8 kg/min dispenser technology
- Another fueling station is opened at candidate location 4 with 3.6 kg/min dispenser technology.

#### 3.2 Fitness of chromosome string solution

The fitness of each chromosome string solution involves several sub-steps. This is summarized as follows:

- Sub-step 1: initialization that translates genetic information of the chromosome into corresponding refueling location decisions
- Sub-step 2: check feasibility and select a path for each O-D pair in all stages
- Sub-step 3: for all feasible O-D pairs determine refueling activities based on the fuel level
- Sub-step 4: for each opened fueling station determine the total number of refueling activities and the corresponding required number of dispensers based on the design level of
- Sub-step 5: calculate the fitness of the chromosome with the objective function described previously

#### 3.3 Population pool

At beginning of the algorithm, we initialized a pool of chromosome strings with a population size of  $N$  (e.g., 500). The pool is defined as the population pool where crossover, mutation, and replacement are applied through an iteration process.

#### 3.4 Parent selection

For each iteration, four candidate chromosomes are randomly selected from the population pool. The four chromosomes are partitioned equally into two groups, and one chromosome will be selected from each group. The chromosome with better fitness (lower objective value) has a better chance to be selected, and the selection

probability is set to be inverse to its objective value. The final selected two parents are defined as  $P_1$  and  $P_2$

#### 3.5 Crossover

The crossover is then applied to the two selected parents ( $P_1$  and  $P_2$ ) to give birth to a new child chromosome  $C$ . Let  $f_{P_1}$  and  $f_{P_2}$  be the objective values of the parents  $P_1$  and  $P_2$ , respectively, and let  $i$  indexes digits of each chromosome,  $i = 1, \dots, |N|$ . Then the chromosome  $C$  is created as follows:

- (1) if  $P_{1i} = P_{2i}$ , then set  $C_i = P_{1i}$  or  $P_{2i}$ ;
- (2) otherwise, then set  $C_i = P_{1i}$  with probability  $p = f_{P_2}/(f_{P_1}+f_{P_2})$ , and  $C_i = P_{2i}$  with probability  $1 - p$ .

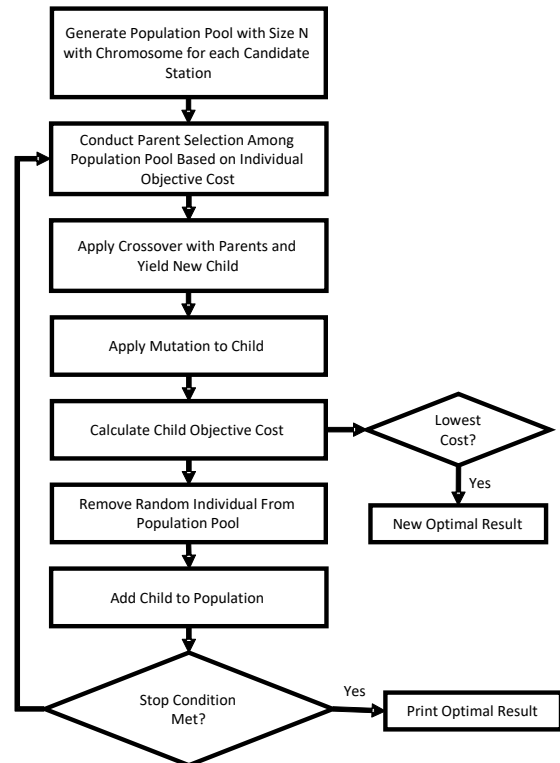
#### 3.6 Mutation

Once a child chromosome  $C$  is created, each element  $C_{i,i} = 1, \dots, |N|$ , has a probability (e.g., 5%) to mutate. Let  $t'$  be a random integer value selected among  $1, \dots, |T|$  with equal probability. If the element  $C_i$  is selected to mutate, then it has two possible ways to change depending on the original value of  $C_i$ :

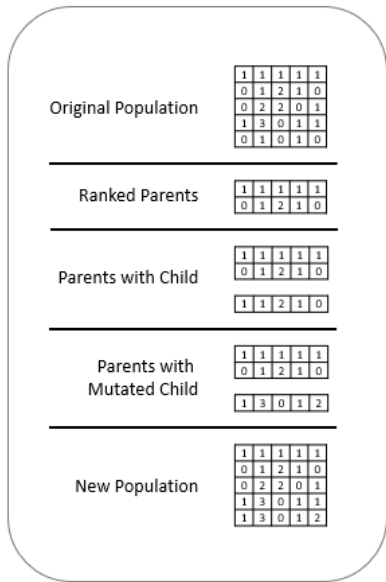
- (1) if  $C_i = 0$ , then set  $C_i = t'$ ;
- (2) otherwise, then set  $C_i = 0$  with probability of 50%, and  $C_i = t'$  with probability of 50%.

#### 3.7 Replacement

After a new individual is added to the population (e.g., a child created with both the crossover and mutation processes), it will replace an existing individual in the population pool. Specifically,  $n$  (e.g.,  $n = 3$ ) candidate individuals are randomly selected from the pool, and the one with the highest objective cost is removed from the pool. The entire genetic algorithm for the problem can be demonstrated using the flow logic and simple example as seen in Figure 28:



(a) GA flow logic and convergence selection



(b) Simple example of chromosome strings and their modifications through various steps of the GA

Figure 28. Flow logic and behavior of the GA

The final solution is the best chromosome achieved with the lowest objective value from the population. Figure 29 shows the number of iterations required to converge on an optimal solution using both the genetic algorithm and iteration process. As shown, many of the solutions converge to near their optimal values within 10,000 iterations which depending on computational power requires about 2-3 minutes per adoption rate.

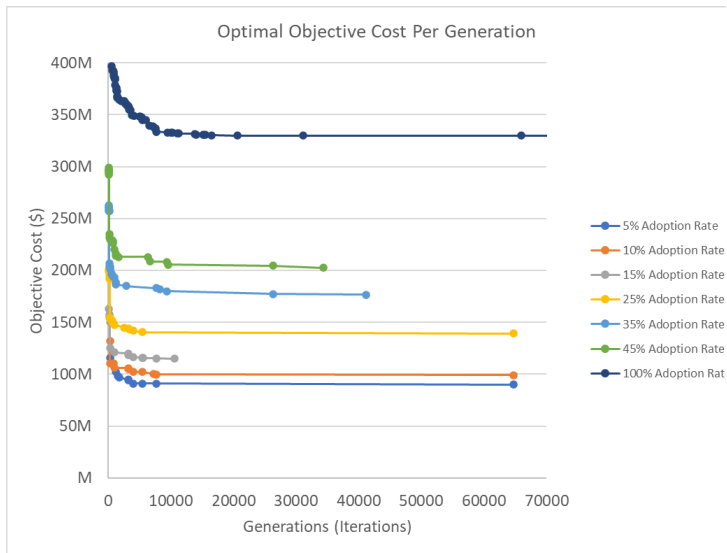


Figure 29. Generations to converge to optimal objective cost

The number of generations for this solution is similar across adoption rates mainly due to the unconstrained locations for implementation of hydrogen refueling stations. In an unconstrained paper, we would expect fewer iterations as the number of potential station locations is reduced by the number of stations in the previous generation.

## Discussion of Results

For the current study, assumptions were made to reduce the complexity of the current model framework and to demonstrate the feasibility of such a model for infrastructure optimization. The

assumptions for the results in this section are as follows:

Table 3. Current Assumptions for Result Generation

Current Assumption	Future Adaptation in Model
All vehicles have a full tank level prior to dispatch. This also assumes that a vehicle can arrive at its destination with less than full tank because it will be refueled prior to being dispatched again	Additional fueling stations and infrastructure can be added along an O-D pair to accommodate refueling off I-75 (or other highway system)
All vehicles were assumed to have a 330 kW FC for this study. Future iterations of OR-AGENT will allow for variable FC sizing depending on vehicle classification.	Allow for a percentage of vehicles in the population to have varying size of FC based on O-D and vehicle class
Tank sizes were assumed to be 100 kg for Class 9-11 and 150 kg for Class 12-13. Realistically, a manufacturer would not create a different tank size for each vehicle unless manufactured at scale. However, without a current co-optimization for distance and fuel tank size this assumption is being made.	Refine the tank size based on real world requirements. This can also be co-optimized based on O-D and vehicle class
Stations can only have a single dispenser technology and all hardware is assumed to be new construction (not upgraded)	Allow for a new cost model to account for multiple dispensing technologies at a station and available upgrade paths for dispensers and other refueling infrastructure
Fuel economy off I-75 is assumed to be the average of the fuel economy on I-75. This assumption allows for the study to not calculate FE on every single route.	Expand the model network to include fuel economy simulations for routes and O-Ds off I-75
Data from Geotab is assumed to be representative of the entire population of heavy vehicles	Add additional data sources to better realize the refueling patterns of vehicles, (i.e. how many actually fill up “outside the fence”) and refueling station demand
A vehicle is assumed to cost approximately \$400,000 and is a loss if not able to make the trip. This is based on the cost of a typical diesel vehicle with appropriate additions to be a FCEV	Allow for varying vehicle costs based on specific architecture
Gross vehicle weight is assumed to be constant throughout the trip, thus fuel economy won’t drastically change based on weight	Allow for some variance, but understanding that the weight will not change significantly throughout the trip unless a vehicle is offloading cargo prior to destination

No traffic or weather data is incorporated currently into the fuel economy calculations	Allow for the additional of weather and traffic data which will likely reduce the overall fuel economy for the vehicles, hence requiring more refueling
Hydrogen is plentiful at each station to accommodate demand. This is incorporated into the cost	Better understand or incorporate methods of transporting or generating hydrogen for refueling to calculate total cost.

For this study, an initial result was generated for a scenario where there are no constraints on what stations can be open or what technologies can exist at any given station, other than the technology must be uniform (no mix of 1.8 kg/min or 3.6 kg/min dispensers at a single location). While this result does not consider all practical facets, it illustrates what the refueling infrastructure requirements would be if, overnight, a certain population of vehicles were to be hydrogen. Input parameters for this result are listed below in Table 4.

Table 4. Parameters Used for Results

Parameter	Description	Default Value
Number of dispenser technologies	Integer value of different dispenser types possible	3
Dispenser flow rate	Array of flow rate in kg/min for each dispenser type	{1.8 3.6 7.2}
Minimum dispensers per Station	Minimum number of dispensers a refueling station must have	2
Maximum dispensers per Station	Maximum number of dispensers a refueling station can have	20
Remaining Fuel Limit	Fuel tank level prior to refilling	20%
Minimum Remaining Fuel Limit	Minimum fuel tank level prior to refilling	5%
Fuel Tank Size	Tank size in kg	Class 9-11: 100 kg Class 12-13: 150 kg
Infeasible Truck Penalty	Cost of a truck not being able to make the trip from origin to destination because fuel level was not sufficient	\$400,000
Technology Adoption Rate	Percent of HD Truck population that is using hydrogen	User Defined

The current primary objective of OR-AGENT is to optimize the location of each refueling station such that the vehicle demand can be met with the lowest possible cost. Optimization of the location of the refueling stations based on refueling requirements is critical to reduce costs, as opposed to building refueling stations at a set uniform location along I-75. Figure 30 shows the optimal result generated by OR-AGENT compared to the unoptimized scenario of every refueling station having a minimum number of dispensers to handle demand. At low adoption rates this illustrates infrastructure cost increases of >67%

of the unoptimized solution as compared with the optimized solution. At high adoption rates we note cost increases of >350% of the unoptimized solution as compared with the optimized solution. Table 5 quantitatively provides a comparison of the total cost between the optimized and non-optimized solutions. Additionally, allowing for not only a dynamic amount of dispensers in parallel with varying dispenser flow rates to manage demand has a large impact on total station cost.

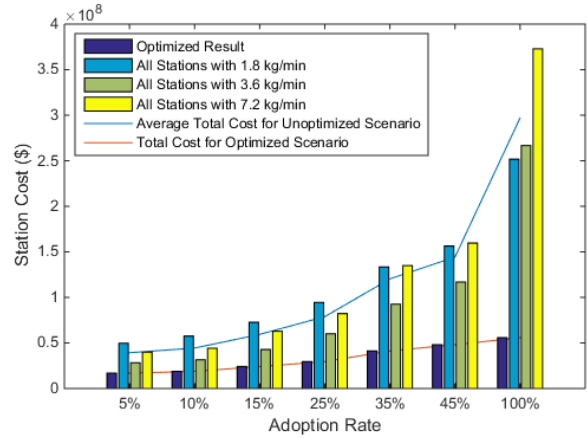


Figure 30. Station Capital Cost

Table 5. Station Cost Optimization

	Optimized Solution Cost	1.8 kg/min Dispensers	Increase from Optimized	3.8 kg/min Dispensers	Increase from Optimized	7.2 kg/min Dispensers	Increase from Optimized
5%	16,833,268	49,707,165	195.29%	28,230,278	67.71%	39,955,762	137.36%
10%	18,806,984	57,553,235	206.02%	31,435,091	67.15%	44,185,944	134.94%
15%	24,093,198	72,636,582	201.48%	42,781,186	77.57%	62,851,917	160.87%
25%	29,519,634	94,448,890	219.95%	60,028,580	103.35%	82,199,322	178.46%
35%	41,275,598	133,480,630	223.39%	92,560,844	124.25%	134,898,772	226.82%
45%	48,092,022	156,392,669	225.19%	116,846,795	142.97%	159,661,705	231.99%
100%	55,750,646	251,725,003	351.52%	266,673,109	378.33%	372,836,921	568.76%

The amount of required fuel for all stations, number of stations required, and the total number of dispensers required for each generation of adoption rate are shown in Figure 31,

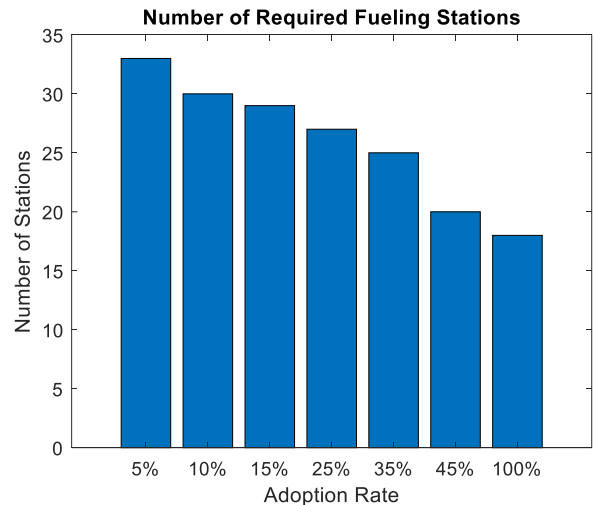


Figure 32, and Figure 33, respectively. Of note, since this is an unconstrained simulation, it was not required that a refueling station remain open, or have hydrogen dispensers, as the adoption rate of hydrogen vehicles increased. Due to this lack of constraint, there are

scenarios where opening a single station in a location can require fewer dispensers at other locations or cause them to close all together. This can be seen in the small increase in requirements for fuel and station cost between the 5% and 10% adoption rates.

Another key finding is that small changes in the technology used in parallel with specific refueling locations can reduce the number of stations required and even reduce the number of dispensers required. For example, the 45% adoption rate requires the most amount of fuel but has the fewest number of total stations. However, this simulation also has the largest amount of 3.6 kg/min dispensers and the only result with a 7.2 kg/min dispenser to handle increased volume.

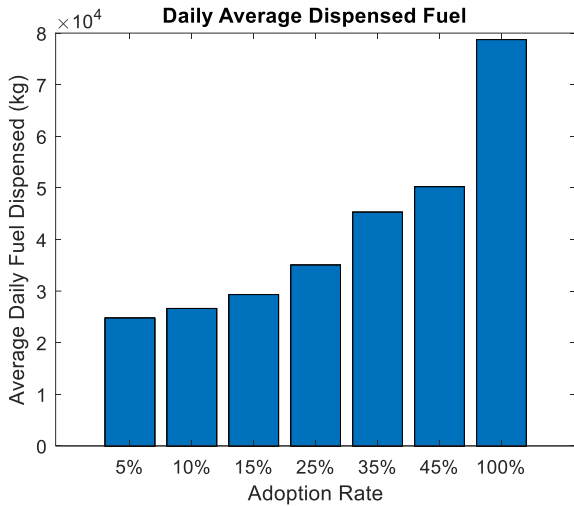


Figure 31. Daily average fuel requirements for each adoption rate

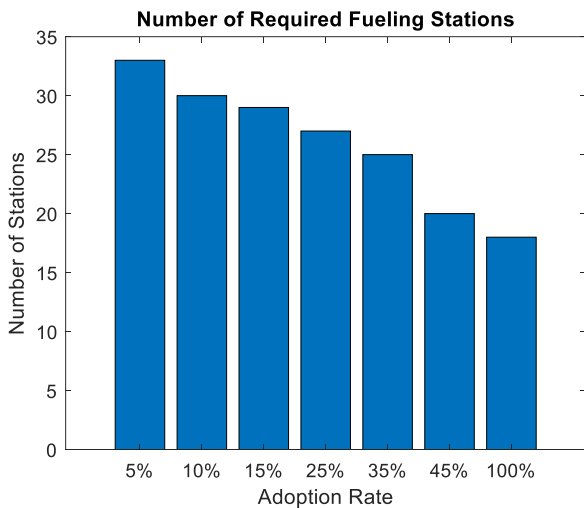


Figure 32. Number of stations required for each adoption rate

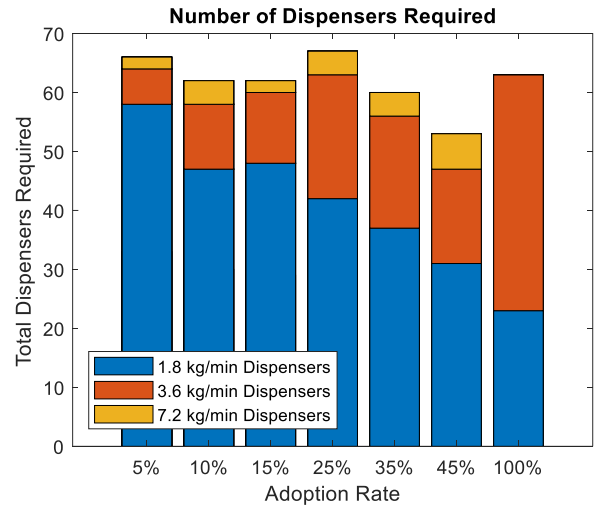


Figure 33. Total dispensers required for each adoption rate

Truck volume, as well as hourly demand, play a large role in where a refueling station is located and how many dispensers are located at that location. In the Figure 34 and

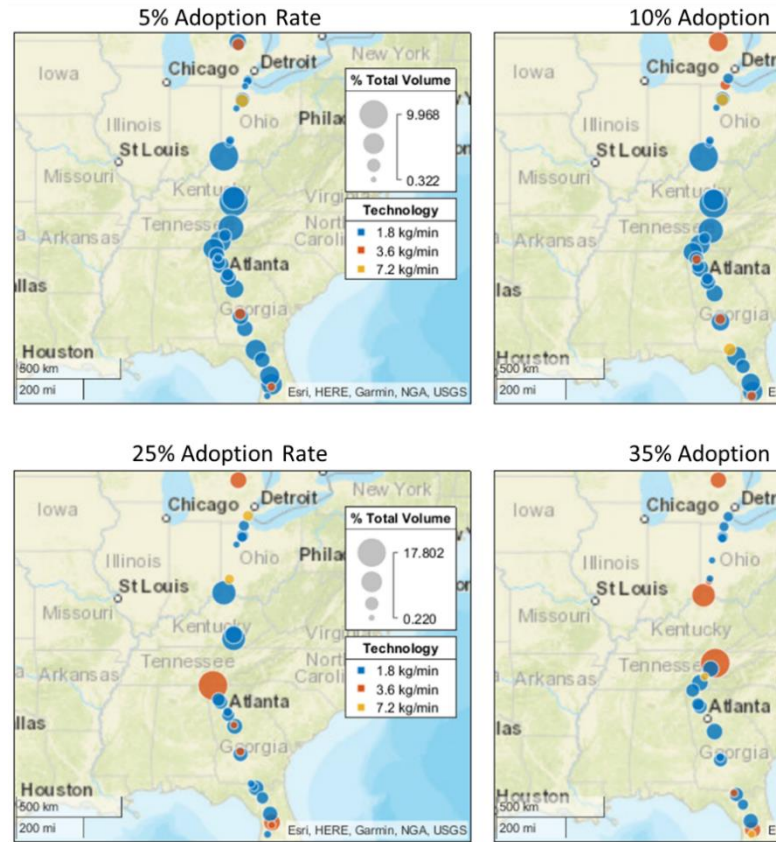


Figure 35, the locations of the refueling stations for each adoption rate are shown with the number of dispensers at each location and the daily truck volume at each location. There are major junctions that have higher volume of trucks, especially near the Tennessee and Georgia border. In part this occurs due to the confluence of several key freight transport corridors, shipping ports, and distribution centers in this region. This is well reflected in the need for additional refueling infrastructure. We expect similar findings on other critical transport corridors where high volume confluences will result in the need for additional refueling infrastructure.



Figure 36 shows the results of each generation of adoption rate for number of stations, daily truck volume per station, and total daily fuel required per station as a function of distance along I-75. Changes between generations are highlighted. This is an unconstrained

simulation, where future studies will refine these results with critical deployment constraints, which would better reflect how a station grows over time when required to remain open.

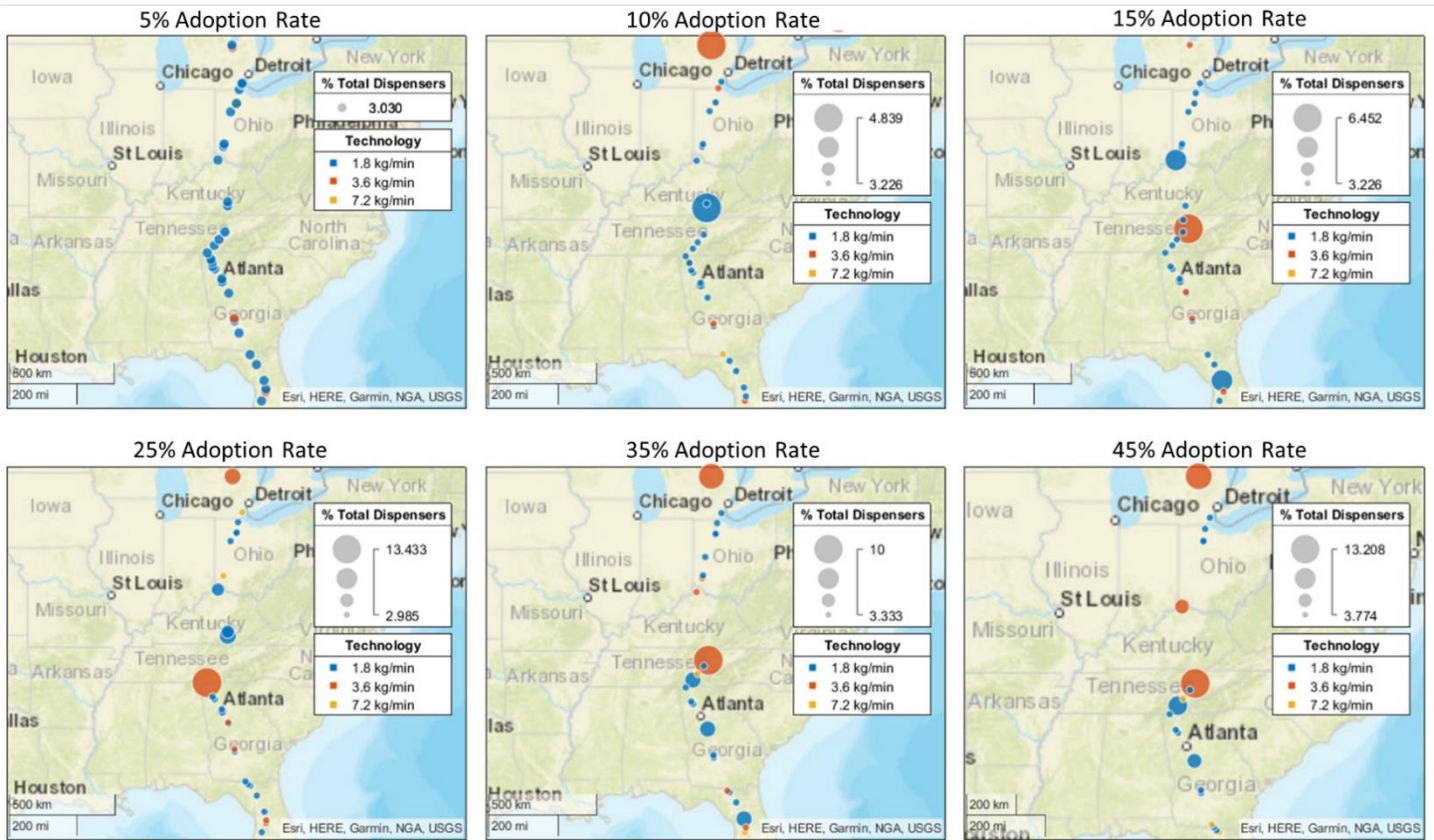


Figure 34. Maps of station sizes at each location scaled to number of dispensers at each candidate site

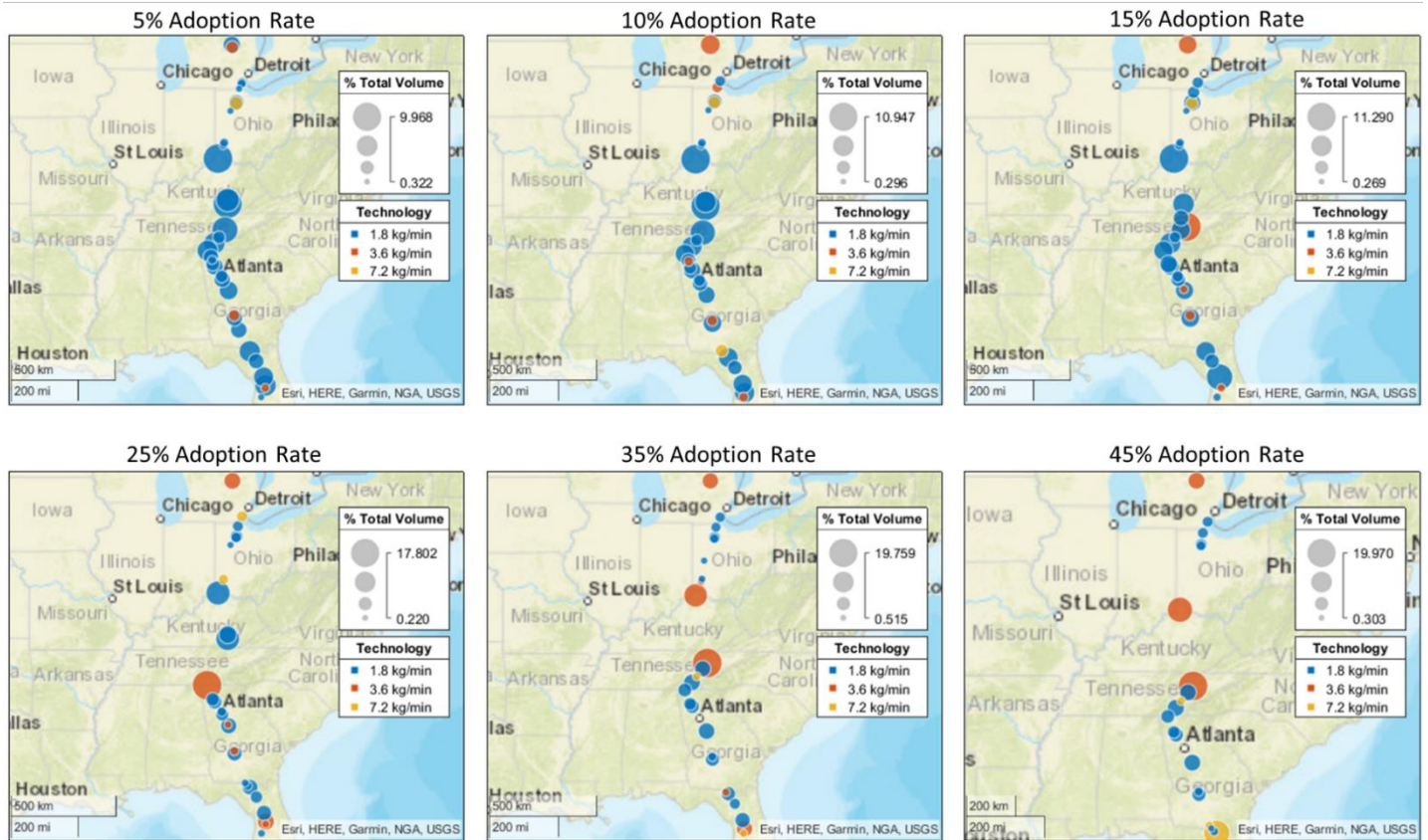


Figure 35. Map of truck volume at each station location

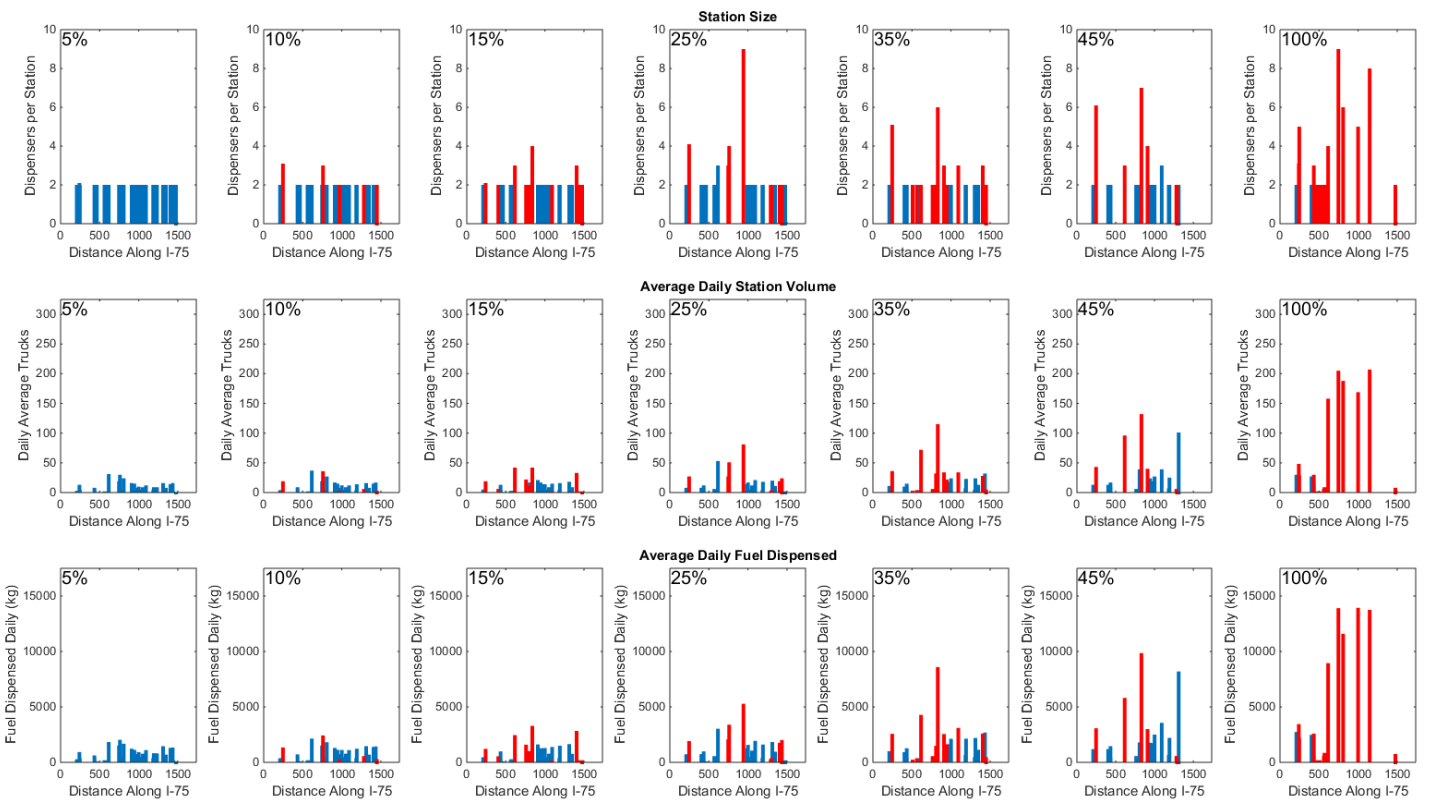


Figure 36. Results of Station size, truck demand and daily fuel requirements for multiple adoption rates (blue – optimum solution, red – change from previous figure generation)

The resulting data from Figure 36 is shown in tabular form in Figure

37. Interestingly, 34 of the 68 candidate stations were never required



be moved, in conjunction with more stations being open for refueling could have many impacts on freight efficiency and how vehicles are produced. Additionally, there are opportunities to explore adding new refueling stations to remote locations to accommodate existing infrastructure, such as the power grid, rather than retrofitting diesel stations to accommodate hydrogen vehicles. More so, safety impact of potential queuing lines at refueling stations, fuel handling, and other areas must be explored.

The results presented only show an example of unconstrained parameters, future papers will focus on a more realistic approach to infrastructure expansion and use of real-world parameters and operational scenarios. The addition of traffic modeling, realistic driver behavior (stopping for lunch etc.) and sources of data show promise in creating an effective tool at designing the future electrified transportation network

## References

- Eckerle, W., Sujan, V., and Salemme, G., "Future Challenges for Engine Manufacturers in View of Future Emissions Legislation," SAE Technical Paper 2017-01-1923, 2017, <https://doi.org/10.4271/2017-01-1923>.
- CARB (2020). Accessed December 20, 2021. <https://ww2.arb.ca.gov/our-work/programs/heavy-duty-low-nox/heavy-duty-low-nox-updates>.
- ICCT (2020). Accessed December 20, 2021. <https://theicct.org/publications/california-hdv-ev-update-jul2020>.
- EPA (2022). Accessed March 31, 2022. <https://www.govinfo.gov/content/pkg/FR-2022-03-28/pdf/2022-04934.pdf>.
- CARB (2019). "Advanced Clean Trucks Regulation," Accessed December 20, 2021. <https://ww2.arb.ca.gov/rulemaking/2019/advancedcleantrucks..>
- Butler, D. (2021). Accessed December 20, 2021. <https://www.washingtonpost.com/climate-environment/2021/03/05/more-than-50-companies-have-vowed-be-carbon-neutral-by-2040>.
- Dean G. (2021). Accessed December 20, 2021. <https://www.businessinsider.com/fedex-delivery-fleet-all-electric-carbon-neutral-2040-sustainability-2021-3>.
- Mathers (2020). Accessed December 20, 2021. <https://business.edf.org/insights/walmart-commits-to-100-zero-emission-trucks-by-2040-signaling-electric-is-the-future>.
- Wikipedia (2021). Accessed December 20, 2021. [https://en.wikipedia.org/wiki/2021\\_United\\_Nations\\_Climate\\_Change\\_Conference](https://en.wikipedia.org/wiki/2021_United_Nations_Climate_Change_Conference).
- DOE (2021). Accessed May 31, 2022. <https://www.energy.gov/articles/us-launches-net-zero-world-initiative-accelerate-global-energy-system-decarbonization>.
- Roeth, M., "Transformational Technologies Reshaping Transportation - An Industry Perspective," SAE Int. J. Adv. & Curr. Prac. in Mobility 3(1):5-48, 2021, <https://doi.org/10.4271/2020-01-1945>.
- NACFE (2020). "Guidance Report: Making Sense of Heavy-Duty Hydrogen Fuel Cell Tractors". North American Council for Freight Efficiency. Report published December 2020.
- Greene, D. L. and Plotkin, S. "Reducing greenhouse gas emission from U.S. transportation". Technical Report; Center for Climate and Energy Solutions: Arlington, VA, 2011.
- Bui A., Slowik P., Lutsey, N. "Power play: Evaluating the U.S. position in the global electric vehicle transition". International Council on Clean Transportation (ICCT), June 29, 2021 Briefing.
- NACAD (2021). Ntl. Acad. of Sciences, Engineering and Medicine. "Assessment of Technologies for Improving Light-Duty Vehicle Fuel Economy—2025-2035". Natl. Acad. Press: DC, 2021.
- Sujan, V.A. "Developing Fuel Cell Electric Powertrain Architectures for Commercial Vehicles". Submitted to the SAE International Journal of Sustainable Transportation, Energy, Environment, & Policy, June 2022.
- Guerrero, A., Davendralingam, N., Raz, A., DeLaurentis, D., Shaver, G., Sujan, V., and Jain, N. "Projecting adoption of truck powertrain technologies and CO2 emissions in line-haul networks". Transportation Research Part D: Transport and Environment, Volume 84, 2020.
- Sujan, V., Xie, F., and Smith, D., "Achieving Diesel Powertrain Ownership Parity in Battery Electric Heavy Duty Commercial Vehicles Using a Rapid Recurrent Recharging Architecture," SAE Int. J. Adv. & Curr. Prac. in Mobility 4(4):1166-1180, 2022, <https://doi.org/10.4271/2022-01-0751>.
- van Grinsven, A.H. et al. 2021, Research for TRAN Committee – Alternative fuel infrastructures for heavy duty vehicles, European Parliament, Policy Department for Structural and Cohesion Policies, Brussels
- Minjares, Ray et al. 2021, Infrastructure to support a 100% zero-emission tractor-trailer fleet in the United States by 2040.
- Uddin, Majbah, Liu, Yuandong, Xie, Fei, Sujan, Vivek, & Siekmann, Adam. Modeling Freight Traffic Demand and Highway Networks for Hydrogen Fueling Station Planning: A Case Study of U.S. Interstate 75 Corridor. United States.
- Liu, Yuandong, Siekmann, Adam, Sujan, Vivek, Uddin, Majbah, Xie, Fei, & Shiqi Ou. Providing Levelized Cost and Waiting Time Inputs for Hydrogen Refueling Station Planning: A Case Study of U.S. I-75 Corridor. United States.
- Xie, F., Lin, Z. (2021). Integrated U.S. nationwide corridor charging infrastructure planning for mass electrification of inter-city trips, Applied Energy, Volume 298, 2021, 117142.
- Hwang, S. W., Kweon, S. J., & Ventura, J. A. (2015). Infrastructure development for alternative fuel vehicles on a highway road system. Transportation Research Part E: Logistics and Transportation Review, 77, 170-183.
- ORNL (2021). <http://faf.ornl.gov/faf5/>. Accessed July 12, 2021.
- Hwang, H. L., Lim, H., Chin, S. M., Wang, R., & Wilson, B. (2019). Exploring the Use of FHWA Truck Traffic Volume and Weight Data to Support National Truck Freight Mobility Study (No. ORNL/TM-2019/1385). Oak Ridge National Lab, Oak Ridge, TN.
- FMCSA (2022). Summary of Hours of Service Regulations. Accessed June 30, 2022. <https://www.fmcsa.dot.gov/regulations/hours-service/summary-hours-service-regulations>.
- FHWA. (2013). Traffic Monitoring Guide.
- Nokia (2022). Accessed June 30, 2021. <https://www.here.com/>.
- Santhanagopalan, S., Smith, K., Neubauer, J., Kim, G-H., Pesaran, A., and Keyser, M. (2014). "Design and Analysis of Large Lithium-Ion Battery Systems". 2014, ISBN: 978-1-60807-713-7
- He, H., Liu, Y., Liu, Q., Li, Z., Xu, F., Dun, C., Ren, Y., Wang, M-X., and Xiea, J. (2013). "Failure Investigation of LiFePO4 Cells in Over-Discharge Conditions". Journal of The Electrochemical Society, 160 (6) A793-A804 (2013)
- Xu, F., He, H., Dun, C., Liu, Y., Wang, M-X, Liu, Q., Ren, Y., and Xiea, J. (2012). "Failure Investigation of LiFePO4 Cells

- under Overcharge Conditions”. ECS Transactions, 41 (39) 1-12 (2012)
33. FPRF (2011). “Lithium-Ion Batteries Hazard and Use Assessment”. Exponent Failure Analysis Associates, Inc., published by the Fire Protection Research Foundation (2011)
  34. Golubkov, A., Fuchs, D., Wagner, J., Wiltische, H., Stangl, C., Fauler, G., Voitic, G., Thaler, A., and Hackere, V. (2014). “Thermal-runaway experiments on consumer Li-ion batteries with metal-oxide and olivine-type cathodes”. Royal Society of Chemistry, RSC Adv., 2014, 4, 3633
  35. Zhang, R., Xia, B., Li, B., Cao, L., Lai, Y., Zheng, W., Wang, H., and Wang, W. (2018). “State of the Art of Lithium-Ion Battery SOC Estimation for Electrical Vehicles”. Energies 2018, 11, 1820.
  36. Geotab (2022). Accessed October 15, 2021. <https://www.geotab.com>
  37. Mintz, M., Gillette, J., Elgowainy, A., Paster, M., Ringer, M., Brown, D., & Li, J. “Hydrogen delivery scenario analysis model for hydrogen distribution options”. Transportation Research Record: Journal of the Transportation Research Board, 1983 (2006), pp.114–120.
  38. Geohash. Accessed July 27, 2022. <https://en.wikipedia.org/wiki/Geohash>.
  39. Vose, M.D., 1999. The Simple Genetic Algorithm: Foundations and Theory. MIT press.
  40. Li, S., Huang, Y., Mason, S.J., 2016. A multi-period optimization model for the deployment of public electric vehicle charging stations on network. Transport. Res. Part C: Emerg. Technol. 65, 128–143.
  41. Li, S., Huang, Y., 2014. Heuristic approaches for the flow-based set covering problem with deviation paths. Transport. Res. Part E: Log. Transport. Rev. 72, 144–158.

<b>kW</b>	Kilowatt
<b>Li-ion</b>	Lithium Ion
<b>LTO</b>	Lithium Titanate
<b>MY</b>	Model Year
<b>NMC</b>	Nickel Manganese Cobalt oxide
<b>NZEV</b>	Near-Zero Emissions Vehicle
<b>O-D</b>	Origin-Destination
<b>OR-AGENT</b>	Optimum Regional Architecture Generation for Electrified National Transport
<b>ORNL</b>	Oak Ridge National Laboratory
<b>REVISE</b>	Regional Electric Vehicle Integrated System Evolution
<b>TCO</b>	Total Cost of Ownership
<b>TMAS</b>	Travel Monitoring Analysis System
<b>WIM</b>	Weight In Motion
<b>ZEV</b>	Zero Emissions Vehicle

## Definitions/Abbreviations

<b>ACT</b>	Advanced Clean Truck
<b>BEV</b>	Battery Electric Vehicle
<b>CARB</b>	California Air Resources Board
<b>CO<sub>2</sub></b>	Carbon Dioxide
<b>DER</b>	Distributed Energy Resources
<b>FAF</b>	Freight Analysis Framework
<b>FC</b>	Fuel Cell
<b>FCEV</b>	Fuel Cell Electric Vehicle
<b>FHWA</b>	Federal Highway Administration
<b>FMCSA</b>	Federal Motor Carrier Safety Administration
<b>GA</b>	Genetic Algorithm
<b>GHG</b>	Greenhouse Gas
<b>H<sub>2</sub></b>	Hydrogen
<b>HOS</b>	Hours of Service
<b>HD</b>	Heavy Duty
<b>HDRSAM</b>	Heavy-Duty Refueling Station Analysis Model

